On Scaling of Hall Effect Thrusters

IEPC-2013-056

Presented at the 33rd International Electric Propulsion Conference,
The George Washington University • Washington, D.C. • USA
October 6 – 10, 2013

Andrey A. Shagayda[1]
Keldysh Research Center, Moscow, 125438, Russia

Abstract: Field of application of Hall effect thrusters is constantly expanding towards increased power and specific impulse and also towards reduced power. Modern level of plasma simulations does not allow accurate prediction of a thruster performance in advance. Therefore the methods of scaling play an important role in creation of new thrusters with desired characteristics. This paper describes an approach to scaling of Hall effect thrusters based on analytical assessments of the discharge plasma parameters and the available experimental data. The approach is based on the observation that in optimized configurations, the discharge channel diameter, its height and length of the ionization zone are changed in the same proportion. On the base of this regularity a semiempirical expression for the anode mass utilization efficiency is obtained. Empirical coefficients of the model are found using an extensive database containing published test results of many thrusters. The obtained expressions allow predicting Hall effect thruster performance for various kinds of propellant when the discharge power and voltage vary in wide range.

Nomenclature

a, a_1, a_3	=	dimensional coefficient in the formula approximating the rate of ionization
a_T	=	coefficient in the approximation the electron temperature as a function of discharge voltage
a_γ	=	coefficient in the approximation the correction factor γ'_q as a function of discharge voltage
$\mathbf{B}$, B	=	magnetic field vector and its modulus, respectively
B_0	=	maximum radial magnetic field on the discharge channel centerline
C, C_1, C_2	=	dimensional coefficients in the expressions of the mass utilization efficiency
C_L	=	proportionality factor between the length of the ionization zone and the channel height
D	=	discharge channel mean diameter
e	=	electron charge
f_e, f_i, f_a	=	velocity distribution function normalized per unit of electron, ion and neutral, respectively
f_{0j}	=	Maxwellian velocity distribution functions of electrons after collision of j th type
g	=	free fall acceleration
G	=	dimensionless criterion of the magnetic field optimality
h	=	discharge channel height
H	=	dimensionless criterion of the magnetic field optimality
I_b	=	beam current
I_d	=	discharge current
I_k	=	ion current of the k th ion species

[1] Leading researcher, Department of Electrophysics, shagayda@gmail.com

I_{spa} = anode specific impulse
k_B = Boltzmann's constant
K_B, K_m = dimensionless similarity criteria
K_q = dimensionless parameter characterizing ion species fraction
L = ionization length
M = atom and ion mass
M_A = relative atomic mass of atoms and ions
m = electron mass
$\dot{m}_a$ = propellant mass flow rate to the accelerating channel
$\dot{m}_b$ = ions mass flow rate
$\dot{m}_k$ = mass flow rate of the k th ion species, k =1,2,3
m_u = atomic mass unit
n_e, n_i, n_a = electron, ion and neutral number density, respectively
n_k = number density of the k th ion species
P_d = discharge power
Q_1, Q_2 = dimensional complexes of variables that determine the value of mass utilization efficiency
$\mathbf{r}$ = radius vector
S = discharge channel cross sectional area
T = thrust
T_e, T_a = electron and atom temperature, respectively
t = time
U_d = discharge voltage
V_e, V_i, V_a = scale of electron, ion and atom velocity, respectively
$\mathbf{v}$ = velocity vector
υ_e = velocity modulus of the electron
α = adjusted dimensional parameter
β_i = ionization reaction rate, $\langle \sigma_i \upsilon_e \rangle$
β_j = reaction rate of j th type of collisions, $\langle \sigma_j \upsilon_e \rangle$
δ = Dirac delta function
γ_E, γ_θ = efficiencies characterizing the spread of ions in velocity modulus and direction, respectively
γ_q, γ_q' = correction factors for the presence of multiply charged ions
ζ_k = number density fraction of the k th ion species, n_k / n_i k =1,2,3
η_a = anode thrust efficiency
η_I = current utilization efficiency
η_m = mass utilization efficiency
η_q = charge utilization efficiency
η_U = voltage utilization efficiency
λ_i = mean free path of atom ionization
μ_k = mass flow rate fraction of the k th ion species, $\dot{m}_k / \sum \dot{m}_k$ k =1,2,3
ξ = exchange parameter
σ_i, σ_{im} = electron-atom ionization cross-section and its maximum value, respectively

σ_j = cross-section of electron-atom j th type collision

ϕ = potential

ΔU = voltage losses

$\Delta\varphi_I$ = potential drop in the ionization region

Ω_k = current fraction of the k th ion species $\Omega_k = I_k \big/ \sum I_k$

I. Introduction

New fields of applications of on-board propulsion systems determine the directions of further improvement of plasma thrusters. These include the growth of specific impulse, increasing the life time, the expansion of the power range, the use of new types of propellant, etc. In particular at present there is increasing interest in electric propulsion systems up to the megawatt power level for use on spacecrafts with nuclear power plant. Hall effect thrusters (HET) are one of the most promising types of electric propulsion to meet these challenges. While expanding the range of operating conditions the forecast of attainable performance of the Hall thrusters is of great interest.

General laws that determine the dependence of Hall effect thruster performance on the discharge power, voltage and type of propellant have been the subject of many investigations, but so far the theory of the discharge in these devices is not complete[1-18]. In particular, there are no reliable calculation methods to determine the maximum possible level of efficiency and specific impulse. In these circumstances the methodologies of scaling play an important role in development of new thrusters with desired performance.

This paper is a continuation and refinement of previous work,[19] devoted to the development of semi-empirical scaling method. Based on the simple physical analysis of the Hall discharge and available experimental data, an expression of the mass utilization efficiency was obtained. In previous work the empirical parameters of this expression were determined using the performance characteristics of the HET SPT-100,[20] and a set of Hall thrusters developed in Keldysh Research Center.[14] In this paper our model is modified by using a collected database of published operating modes of more than thirty thrusters. At present the database contains the operating modes of the following thrusters: SPT-25,[21] SPT-30,[22] SPT-50,[23] SPT-70,[24] SPT-100,[20,25-27] SPT-115,[28] SPT-140,[25,29,30] PPS®X00,[31] PPS-1350,[32,33] PPS®X000,[34,35] BHT-200,[36,37] BHT-600,[38,39] BHT-1000,[40] BHT-1500,[41,42] BPT-4000,[43-45] BHT-8000,[46] BHT-20K,[47] NASA-103M.XL,[48] NASA-120M,[49] NASA-HiVHAc,[50,51] NASA-173,[52-54] UM/AFRL P5,[52] H6,[55] NASA-T-220,[56] NASA-300M,[57] NASA-400M,[58] NASA-457,[59-61] MELCO's 200 mN,[62] HT-100,[63] KM-32,[64] KM-45,[65] KM-60,[66,67] KM-88,[66,67] KM-7M.[66] The database contains modes of operation on xenon, krypton, argon, iodine and zinc. Figure 1 shows anode specific impulse as a function of the discharge power at all operating points, containing in the database.

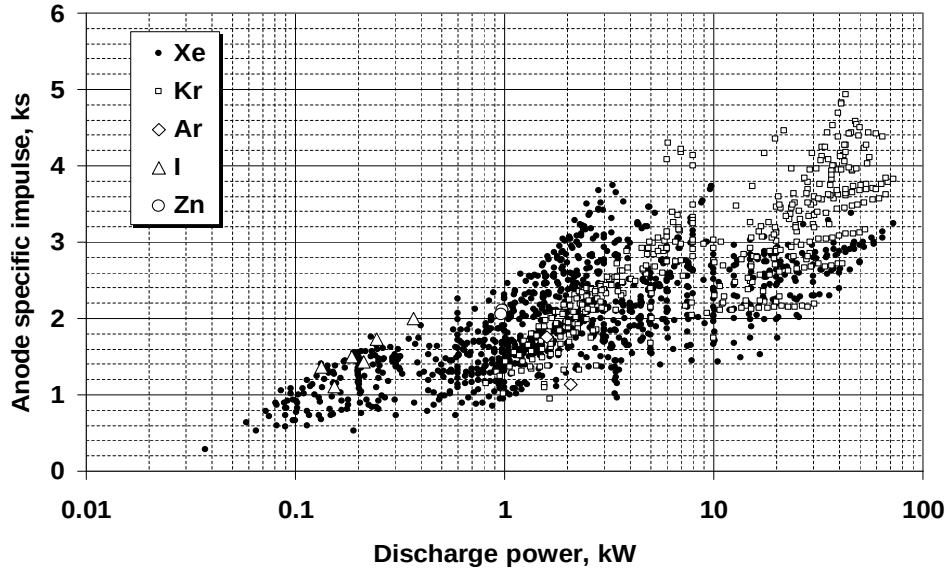

Figure 1. Anode specific impulse as a function of the discharge power of HETs, containing in the database.

A set of parameters characterizing the thruster's geometry and modes of operation includes the following values: the mean diameter of discharge channel, the height of the channel, discharge power, discharge voltage, anode mass flow rate and thrust. From these data, the anode specific impulse, anode efficiency and a number of other ancillary values are calculated. Not all of the publications contain a comprehensive set of needed data. In particular, some articles present data on full propellant flow rate, including the flow into the cathode, or the data of the full specific impulse. In this case, the anode characteristics were calculated on the assumption that the share of the cathode mass flow rate is 10% of the total mass flow rate. This introduces some uncertainty in the data. A significant part of articles contains no data in tables, but in graphs. It also brought a certain error in collected data. In the current state the database does not contain information on the thrusters with anode layer. In the future, the database will be updated and supplemented.

The remainder of this paper is organized as follows. The basic ideas of the approach to scaling are described in Section II. This section explains which assumptions of the scaling model do not contradict to experimental data and why scaling can not make full use of the similarity criteria. The problem of similarity is considered in section III. The possibility of use a similar reduced model to estimate the output characteristics and lifetime of a Hall thruster with high power is analyzed. The latter task is very important due complexity and high cost of the full-scale tests of high power Hall effect thrusters. The problem of prediction of achievable parameters while scaling Hall effect thrusters is considered in sections IV-V. The idea that optimized thrusters should be geometrically similar is put forward. Performance parameters are estimated on the basis of semiempirical expressions for mass utilization efficiency and charge utilization efficiency. This makes it possible to quantitatively explore the patterns of performance changes when changing the size, discharge power, voltage and type of propellant.

II. Approach to Scaling

Since the early studies devoted to scaling problem, the thesis was put forward that in order to derive scaling laws, it is necessary to use the criteria of similarity. Apparently the first paper, devoted to the study of Hall effect thrusters similarity,[1] has introduced a dimensionless similarity criterion λ_i / L, where $\lambda_i = V_a / \left(\langle \sigma_i \upsilon_e \rangle n_e \right)$ is the mean free path to the ionization of an atom, L is the length of the discharge channel, V_a is the characteristic velocity of atoms, n_e is the electrons number density, $\langle \sigma_i \upsilon_e \rangle$ is the ionization reaction rate i.e. the product of the ionization cross-section σ_i to the electron velocity υ_e, averaged over electron velocity distribution function. This parameter characterizes the probability of ionization of neutral atoms in the discharge channel and eventually the propellant mass utilization efficiency. Later it was offered to name it *Melikov–Morozov criterion*.[2] Most scaling approaches are based on the trying to ensure the invariance of the Melikov-Morozov criterion.

V. Khayms and M. Martinez-Sanchez studied the variant of photographic scaling at which the diameter of the channel, the height and length of the ionization zone are reduced in the same proportion.[3] They noted that to maintain a constant probability of ionization in the discharge channel it is required to increase the density of the plasma, and this will lead to an increase in heat flux on the channel walls and reduction of the lifetime. V. Kim and co-workers in the development of low-power Hall thrusters used the same idea.[4]

E. Ahedo and J. Gallardo have noted that there is a problem of magnetic saturation, increasing the flow of heat and reducing the lifetime when applying a photographic scaling.[5] As an alternative solution to preserve the probability of ionization they proposed to reduce the sectional area of the channel, keeping unchanged the length of the ionization zone.

M. Andrenucci and co-workers argued that the common limit of all previous approaches is that the scaling of the channel radius is not treated separately from the other radial dimensions, which means the scale and shape effects are mixed.[6] They tried to use a more systematic approach, treating each geometrical parameter separately. The same approach, supplemented by an extensive database covering many different HETs, was applied by F. Battista and co-workers[7] and T. Misuri and co-workers[8] to find design dimensions of a set of high power thrusters.

J. Ashkenazy and co-workers looked for the ways of changing the different sizes of channel for efficient work at reduced power, aiming to achieve the invariance of the Melikov-Morozov criterion.[7] They showed that scaling down the channel size have a consequences of increased power losses and reduced overall thruster efficiency. To avoid these effects they proposed an alternative approach that consists in extending the channel length at constant area of the channel cross-section.

K. Dannenmayer and S. Mazouffre used the database and also took, as the basis, condition of invariance of the Melikov-Morozov criterion, using the assumption that the length of the ionization zone, the height and diameter of the channel can be changed independently.[8]

In our opinion, the drawback of most studies is that they ignore the following two experimentally established facts: first, the length of the ionization zone is not an independent quantity, and is close in magnitude to the height of the channel, and secondly, in the optimal configuration the height of the channel is proportional to its diameter. The disadvantage of works in which these facts are not ignored, is an attempt to keep the invariance Melikov-Morozov criterion. Let us examine these theses in more detail.

As is known, the Hall thruster efficiency can be represented as the product of a set of dimensionless parameters, describing the different types of losses.[9] Therefore the earlier studies have tried to find the relationship between the anode efficiency and dimensionless similarity criteria of the discharge. One of the first phenomenological models[2] included the following performance coefficients: mass utilization efficiency $\eta_m = \dot{m}_b/\dot{m}_a$; voltage utilization efficiency $\eta_U = 1 - \Delta U/U_d$, where ΔU is voltage losses; the so-called "exchange parameter" $\xi = I_d/(e\dot{m}_a/M)$, (in later publications the current utilization efficiency $\eta_I = I_b/I_d$ is usually used). This model did not take into account multiply charged ions. The parameters η_m, ΔU and ξ, were measured in five different Hall effect thrusters with channel diameter from 50 to 200 millimeters. The authors have tried to find the only parameter on which depend all the dimensionless parameters. They were looking for it in the form $\alpha = [\dot{m}_a/S]\cdot h^k$, where S is the channel cross sectional area, h is the channel height, and k was adjustable exponent. This parameter was varied so that the experimentally measured dependencies of $\eta_m(\alpha)$, $\Delta U(\alpha)$ and $\xi(\alpha)$ were approximately the same for all thrusters. It was found that the best match is achieved at $k = 1$, i.e. dimensionless efficiency parameters of all thrusters with good accuracy are functions of the dimensional value $\alpha = \dot{m}_a/(\pi D)$. Therefore it was hypothesized that this parameter can be expressed through the dimensionless scaling parameters of the discharge. Tests of this assumption showed that the parameter α can be expressed in terms of the Melikov–Morozov criterion in case if $L = h$. In other words, the experiments showed that the length of ionization zone is approximately equal to the height of the channel and not the distance from the anode to the channel exit plane.

Apparently, the Ref. 2 is the first in which it has been experimentally found that the length of the ionization zone is not equal to the length of the discharge channel. In the Ref. 2 it was suggested that this feature is connected with using of narrow magnetic poles, and the length of the ionization zone is determined by the topology of the magnetic field. Subsequently, the statement that in the Hall thrusters with an optimized magnetic field the ionization length is approximately equal to the length of region with a large magnetic field, and this length in turn is approximately equal to the height of the discharge channel, i.e. $L \approx h$, was repeated in a review article by V. Kim.[9] In recent years, evidence that region with intensive ionization roughly coincides with the region of high magnetic field were obtained both in the probe measurements (see, for example, measured and calculated distributions of plasma parameters presented in Ref. 10) and in the numerical simulations.[11]

Experience shows that approximate equality $L \approx h$ is not the only limitation that must be taken into account when scaling Hall thrusters. Analysis of a large number of different thrusters indicates that the two dimensions D and h in optimized thrusters are approximately proportional to each other. For example, K. Dannenmayer and S. Mazouffre have analyzed the data base containing information of a series of 33 different single-stage Hall thrusters, and pointed to this regularity.[12] They suggested that this result could be explained by the fact, that the usual geometry of modern Hall thrusters is an extrapolation of the design of the Russian Hall effect thruster SPT-100.[13] In our view, there are deeper reasons.

Keldysh Research Center has developed several Hall thrusters in the power range from 200 W to 5 kW, with a nominal discharge voltage from 250 V to 700 V.[14] Four of these thrusters were brought to the level of the flight model. Several more of engineering and laboratory models have been worked out and passed life tests lasting from 500 to several thousand hours. Because of the lack of reliable modeling methods when creating these thrusters the required performance characteristics have been achieved experimentally. During the development of thrusters, the diameter and height of the discharge channel were independently altered, by every possible ways. For each ratio of the channel height to diameter, several variants of the magnetic system were tested. In these studies, it was found that the optimum operating conditions are achieved for all thrusters at approximately the same ratio of channel height to diameter. These studies also have shown a correlation between thruster efficiency and the dimensionless criteria G and H.[15,16] These criteria characterize the average of the magnetic mirror ratio, which affects the frequency of electron collisions with the walls of the discharge channel. It is important to note that the invariance of these criteria is provided by the similarity of the spatial distributions of the magnetic field, and by the similarity of the channel geometries, i.e. provided $h \sim D$. Deviations from this similarity that occur when changing h and D in different proportions lead to a reduction of the dimensionless criteria and worsening of thruster performance. The

efficiency of the dimensionless criteria was also confirmed in the experiments presented by A. Loyan and T. Maksymenko.[17]

Thus, available experimental data suggest that the scaling model must take into account the relations $L \approx h$ and $h \sim D$ i.e., it should be based on the so-called "photographic" scaling of all linear dimensions. But in this case, when reducing the size of the thruster, it is difficult to achieve invariance of the Melikov-Morozov criterion. Trying of keeping this value, leads to problems of increased heat flow on the walls and fall of the thruster lifetime. These problems were already mentioned in earlier works,[18] as well as in almost all the above cited studies on the problem of scaling. On the other hand, when increasing power, the desire to preserve the invariance of the Melikov-Morozov criterion is meaningless, since in more powerful thrusters the probability of ionization and mass utilization efficiency can be increased. Therefore, the task of ensuring the similarity of the physical processes and the task of HET's scaling should be considered separately. The task of ensuring similarity can be considered, for example, when we want to create a small similar model and use it to determine the characteristics of a more powerful thruster. In the problem of scaling we can not demand similarity of the physical parameters, such as Melikov-Morozov criterion. In our approach we tried to investigate these two different tasks on the basis of experimentally established relationships $L \approx h$ and $h \sim D$.

III. Discharge Similarity Criteria

The analysis of similarity laws usually bases on the consideration of the hydrodynamic equations of plasma. In our view in this case the number of possible dimensional and dimensionless parameters, which can provide a similarity, is too large, and their choice is somewhat arbitrary (see for example Ref. 67). In the pioneer work of A. Morozov and I. Melikov the similarity criterion was obtained using kinetic equation for ion and neutral particles.[1] The use of a single kinetic equation instead of a whole set of hydrodynamic equations allows obtaining a minimum set of similarity criteria in the most general case. In addition, the use of kinetic equations allows avoiding additional assumptions about the nature of the viscosity and thermal conductivity, which are required to withdraw hydrodynamic equations.

However the similarity criteria, obtained by A. Morozov and I. Melikov, are inconvenient to use, as it was noted, for example, in Ref. 68. In our opinion this is the result of not quite right choice of scale for ion velocity. It was chosen equal to the thermal velocity of the neutral atoms that move a few orders of magnitude slower than ions. Besides, in deriving criteria, the kinetic equation for electrons was not used. It seems more logical, when deriving similarity criteria, to use kinetic equations for electrons, ions and neutral atoms, and to choose separate characteristic velocities for each type of particles.

Consider the quasi-neutral plasma, consisting of electrons, singly charged positive ions and neutral atoms. Kinetic equation of electrons with collision integrals in the form of Krook, neglecting Coulomb and recombination collisions can be written as[69]

$$\frac{\partial(n_e f_e)}{\partial t} + \mathbf{v}\frac{\partial(n_e f_e)}{\partial \mathbf{r}} + \frac{e}{m}\left(\frac{\partial \phi}{\partial \mathbf{r}} - \mathbf{v}\times\mathbf{B}\right)\frac{\partial(n_e f_e)}{\partial \mathbf{v}} = \beta_i n_a n_e f_{0i} + n_a n_e \sum_j \beta_j \left(f_{0j} - f_e\right). \quad (1)$$

The first term of the right-hand side of Eq. (1) describes the appearance of the secondary electrons as a result of ionization. The second term is the sum of the collision integrals, describing the change of the distribution function of primary electrons in elastic and excitation collisions with neutral particles. In Eq. (1) we also assume that the magnetic field is external, and use a potential to describe the electric field. Here and below we use the distribution functions, normalized to unity, because the conversion of kinetic equations to dimensionless form thus becomes easier.

Let us introduce the following velocity scales for the plasma components: $V_e = U_d/(hB_0)$ is the characteristic electron drift velocity in crossed fields; $V_i = \sqrt{2eU_d/M}$ is the characteristic velocity of the ions moving in a quasi-stationary electric field with a potential difference of the order of discharge voltage; $V_a = \sqrt{k_B T_a/M}$ is the characteristic thermal velocity of neutral atoms with temperature T_a. Using these characteristic velocities we can transform Eq. (1) to dimensionless form by making the following change of variables (dimensionless quantities are marked with primes):

$$\phi = U_d\,\phi',\ \mathbf{B} = B_0\,\mathbf{B}',\ \mathbf{r} = h\,\mathbf{r}',\ \mathbf{v} = V_e\,\mathbf{v}',\ t = \left(h/V_e\right)t',\ \beta_j = \sigma_{im} V_e\,\beta_j',$$

$$f_e = f_e'/V_e^3,\ f_{0j} = f_{0j}'/V_e^3,\ n_i = n_e = \frac{\dot{m}_a}{\pi DhMV_i} n_e',\ n_a = \frac{\dot{m}_a}{\pi DhMV_a} n_a'. \tag{2}$$

Here we used the condition of quasi-neutrality. For the scale of the plasma number density we took the ratio of the atoms flow density to the characteristic velocity of the ions. The use of atoms flow density instead of ions flow density is justified, since about 90% of propellant atoms in the effectively working average power Hall thrusters are converted into ions. Carrying out in Eq. (1) indicated change of variables, we obtain equation

$$\frac{\partial\left(n_e' f_e'\right)}{\partial t'} + \mathbf{v}'\frac{\partial\left(n_e' f_e'\right)}{\partial \mathbf{r}'} + K_B\left(\frac{\partial \phi'}{\partial \mathbf{r}'} - \mathbf{v}'\times\mathbf{B}'\right)\frac{\partial\left(n_e' f_e'\right)}{\partial \mathbf{v}'} = K_m n_a' n_e'\left[\beta_i' f_{0i}' + \sum_j \beta_j'\left(f_{0j}' - f_e'\right)\right] \tag{3}$$

in which two dimensionless parameters are introduced:

$$K_B = \frac{eh^2 B_0^2}{mU_d},\qquad K_m = \frac{\dot{m}_a \sigma_{im}}{\pi DMV_a}. \tag{4}$$

Here it would be necessary to use the condition $h \sim D$, but we have kept the two separate values to criteria had a more familiar look.

The two parameters in Eq. (4) contain practically all the important dependence obtained earlier in studies of the similarity laws. For example, at a fixed height of the channel ($h = const$) to ensure the invariance of K_B the magnetic field should vary according to the well known law $B_0 \sim \sqrt{U_d}$ obtained earlier in the hydrodynamic approximation by V. Erofeev and A. Zharinov[70]. At $U_d = const$ from $K_B = const$ we find also known relation $B_0 \sim h^{-1}$ observed in experiments[9]. The invariance of the parameter K_m for a given sort of propellant ($\sigma_0 = const$) at a constant thermal velocity of neutral atoms ($V_a = const$) leads to the relation $\dot{m}_a/\pi D = const$, which corresponds to experimental data[2] and is a consequence of approximate equality $L \approx h$, as it was noted above. One can also see that combination $\sqrt{2m/M}\left(\sqrt{K_B}/K_m\right)$ equals to the Melikov-Morozov criteria if we take into account, the electrons characteristic velocity $V_e = U_d/\left(hB_0\right)$.

The right-hand side of Eq. (3) is the sum of terms describing elastic, ionization and excitation collisions. Each of the reaction rate of *j*th type of collision in the right-hand side of the kinetic equation in dimensionless variables can be written as

$$\beta_j' = \iiint |\mathbf{v}'|\sigma_j'\left(|\mathbf{v}'|\sqrt{\frac{eU_d}{mK_B}}\right) f_e'(\mathbf{v}')\,d\mathbf{v}'. \tag{5}$$

From this expression we can see, that the invariance of the sum of the model collision integrals is possible only when $U_d = const$. The other words, strict similarity is attainable only at the same discharge voltage.

The kinetic equation for ions can be written as

$$\frac{\partial\left(n_i f_i\right)}{\partial t} + \mathbf{v}\frac{\partial\left(n_i f_i\right)}{\partial \mathbf{r}} - \frac{e}{M}\frac{\partial \phi}{\partial \mathbf{r}}\frac{\partial\left(n_i f_i\right)}{\partial \mathbf{v}} = \beta_i n_a n_e \delta(\mathbf{v}). \tag{6}$$

Here we assume that the velocity of ions at the time of their appearing is zero, the influence of magnetic field on the motion of ions can be neglected and the ions move without collisions. Using the same scales for distances, potentials, and particle numerical densities, as in the equation for the electrons, we choose for ions the typical

velocity scale $\mathbf{v} = V_i \mathbf{v}'$ and typical time scale $t = (h/V_i)t'$. As a result, we obtain the dimensionless kinetic equation for ions:

$$\frac{\partial(n_i' f_i')}{\partial t'} + \mathbf{v}' \frac{\partial(n_i' f_i')}{\partial \mathbf{r}'} - \frac{1}{2} \frac{\partial \phi'}{\partial \mathbf{r}'} \frac{\partial(n_i' f_i')}{\partial \mathbf{v}'} = \left(\frac{K_m}{\sqrt{K_B}} \sqrt{\frac{M}{2m}} \right) \beta_i' n_a' n_e' \delta(\mathbf{v}') \cdot \tag{7}$$

The factor in the round brackets of the right part of the equation, is reciprocal of the Melikov-Morozov criterion. We can see that in the invariance of K_B and K_m the similarity of ion fluxes is achieved only for a given propellant ($M = const$). If for neutral atoms we choose velocity scale V_a, and time scale h/V_a, we obtain dimensionless kinetic equation

$$\frac{\partial f_a'}{\partial t'} + \mathbf{v}' \frac{\partial f_a'}{\partial \mathbf{r}'} = -\left(\frac{K_m}{\sqrt{K_B}} \sqrt{\frac{M}{2m}} \right) \beta_i' n_e' f_a', \tag{8}$$

that does not add a new similarity criteria.

In our analysis, we did not touch the boundary conditions, the account of which should lead to additional criteria, containing such parameters as the scale of the roughness, coefficient of secondary electron emission and some others. This aspect is quite complex and requires a separate study.

From the above analysis we can conclude that the similarity of the plasma parameters can be obtained only by fairly rigid restrictions: two thrusters should have a geometrically similar discharge channels, and the magnetic field configuration and must operate at the same discharge voltage and on the same type of propellant. There is only one way to ensure that similarity: in geometrically similar Hall thrusters on the same kind of propellant at equal discharge voltages make $B_0 \sim h^{-1}$ that ensures the invariance of the parameter K_B, and make $\dot{m}_a \sim D$ for the invariance of K_m. However in this case there are problems associated with the heat flux on the discharge channel walls, as it was noted above. The heat flux density increases when reducing the size of the thruster and keeping the probability of ionization. Therefore, to ensure the strict similarity at least one of the thrusters should have a means of forced heating (or cooling) of the walls. Another problem is associated with reducing the size of the magnetic system. Firstly, size reduction can lead to magnetic saturation. Secondly, the similarity condition $B_0 \sim h^{-1}$ requires increasing of the current density in magnetic coils and may require additional cooling of the windings.

Thus, the problem of full-scale simulation of the Hall thruster operation using a thruster with reduced size is extremely complex, but, in principle, is feasible under the condition of forced cooling of both the discharge channel ceramic walls and magnetic coil windings. The technical realization of forced cooling could solve an extremely important problem of the organization of the accelerated life tests. Taking into account high complexity and high cost of direct life tests, such modeling can dramatically reduce the cost and time of experimental testing of the Hall thrusters, and when creating thrusters with power of tens and hundreds of kilowatts, may become perhaps the only way of experimental confirmation of lifetime characteristics.

IV. Regularities of Scaling

A. Scaling of Linear Dimensions

The purpose of scaling is ensuring of the highest possible performance when creating a new thruster, which may differ from the prototype by power, discharge voltage and type of propellant. As was mentioned above, to achieve this goal we can not demand the preservation of the ionization probability. We must demand that the heat flux to the walls remained within reasonable limits, and there was a required lifetime. And we should be able to estimate, what will be the probability of ionization, as well as other non-dimensional performance parameters, in the given mode of operation. Taking into account the results of numerous experiments, we will assume that the optimal configuration corresponds to the requirements of the “photographic” scaling. Therefore in order to obtain the scaling model, we need to find a common scaling factor of all linear dimensions for given discharge power, discharge voltage and kind of propellant and then evaluate the achievable performance.

Analysis of the available statistics on Hall effect thrusters shows, that in the first approximation, the linear size of the channel is proportional to square root of the discharge power. Figure 2. shows channel mean diameters as a function of the nominal discharge power for different Hall thrusters from the collected database. Also, the graph shows two functions: solid line is a trend approximation of the data by a power function, and dashed line is the trend approximation by the function proportional to square root of the discharge power. In the presented formulas the discharge power is expressed in kilowatts and the diameter in millimeters. This relationship has a well known simple explanation. When creating new thrusters developers assume that the share of power losses on channel walls is approximately the same in all optimized thrusters. Therefore, to maintain the density of the heat flux on channel walls at the same level, it is necessary to provide the relation $D \sim \sqrt{P_d}$. In our model, we also will assume that the similarity coefficient of linear dimensions is determined only by the discharge power. The next step is to calculate the achievable performance parameters.

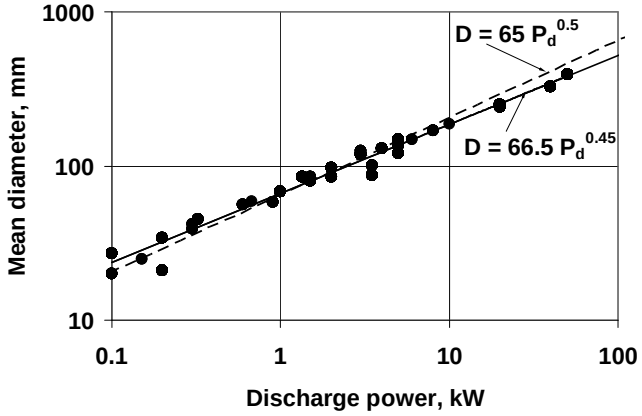

Figure 2. Channel mean diameter as a function of the discharge power for a variety of HETs.

B. Phenomenological Performance Model

The main parameters characterizing the efficiency of the anode unit of a Hall thruster, are the anode efficiency

$$\eta_a = T^2/\left(2\dot{m}_a P_d\right) \tag{9}$$

and anode specific impulse

$$I_{spa} = T/\left(\dot{m}_a g\right). \tag{10}$$

These values can be represented as products of several coefficients that describe the various types of losses. There are several ways of such representation, which differ mainly in the method of describing of the losses due to dispersion of the ion velocity distribution function and the presence of multiply charged ions in the accelerated plasma.[71] Here we will use the following loss factors which were investigated in Ref. 72:

the mass utilization efficiency

$$\eta_m = \left(\sum \dot{m}_k\right)/\dot{m}_a\,, \tag{11}$$

where $\dot{m}_k$ is mass flow rate of *k*th species;

the current utilization efficiency

$$\eta_I = \left(\frac{e}{M}\sum k\dot{m}_k\right)\Big/ I_d\,, \tag{12}$$

where the numerator is the total current of ions;

the voltage utilization efficiency

$$\eta_U = \gamma_E^2\gamma_\theta^2\,, \tag{13}$$

where coefficient γ_E characterizes the loss due to the energy distribution of ions, the coefficient γ_θ characterizes the loss due to the beam angular distribution, and a product $\gamma_E\gamma_\theta$ is the ratio of actual to ideal thrust, which would create the accelerated ions, if they are moving parallel to the axis of the thruster and have the same energy, corresponding to the discharge voltage;

the charge utilization efficiency

$$\eta_q = \gamma_q^2 / \gamma_q' , \tag{14}$$

where

$$\gamma_q = \sum \sqrt{k}\,\mu_k , \tag{15}$$

$$\gamma_q' = \sum k\mu_k , \tag{16}$$

Here μ_k is mass flow rate fraction of the k th ion species:

$$\mu_k = \dot{m}_k / \sum \dot{m}_k . \tag{17}$$

If we assume that ions with different multiplicity have similar velocity distributions, the anode efficiency and anode specific impulse can be expressed as[72]

$$\eta_a = \eta_q \eta_m \eta_I \eta_U , \tag{18}$$

$$I_{spa} = \gamma_q \eta_m \sqrt{\eta_U} \sqrt{\frac{2eU_d}{Mg^2}} . \tag{19}$$

To predict the characteristics of the thruster, it is necessary to find out how these factors depend on the thruster size and mode of operation.

Research experience,[71-73] shows that at change of discharge power, discharge voltage and kind of propellant, the most significant changes occur with mass utilization efficiency. In addition the specific impulse is appreciably affected by the ions species fraction. Effect of changes in other factors on performance is weaker or has no explicit dependence on the parameters of the work.

A series of measurements, undertaken at the Keldysh Center for a number of Hall effect thrusters with rated power from 200 W to 2 kW, did not show any well-defined correlation between the value of η_I and the thruster's operating mode. For different thrusters, different characters of this value change with the discharge power and discharge voltage were observed. The typical values of this parameter for all thrusters were in the range 0.70…0.80. Therefore, in the absence of more reliable information, in the subsequent calculations we will use the approximation $\eta_I \approx const$.

In the conducted experiments the coefficient γ_θ usually increased slightly with discharge power, while remaining within the range of 0.94…0.95. There was also a weak dependence of the energy coefficient γ_E on the discharge voltage, and it is usually in the range 0.93…0.95. Therefore the value of voltage utilization efficiency $\eta_U = \gamma_E^2\gamma_\theta^2$ was usually in the range 0.76…0.82. All these results were obtained on xenon. It should be noted that J. L. Linnel in the investigation of krypton[52] has found that the beam divergence efficiency is approximately 8% better for xenon than for krypton. It is not known what caused this difference. Perhaps there are fundamental physical reasons; perhaps it is necessary to optimize the magnetic system differently for xenon and krypton. Due to the lack of sufficient data, in this work we assume that the coefficients γ_θ, and γ_E are approximately constant and therefore $\eta_U \approx const$.

According to Eq. (18) the maximum anode efficiency at given data should be less than ~0.65. Figure 3 shows the anode efficiency as a function of the discharge power for different HETs in the database. It is seen a presence of operation modes with anode efficiency up to 0.71…0.72. The most likely explanation is that at increased discharge power and voltage, or by better optimization of the thruster design, the losses associated with the energy and angular spread of ions can be reduced. Therefore we will assume, that in optimized Hall effect thrusters, the considered loss factors may reach the values of η_I=0.8; η_U=0.9, and the measured values of η_I=0.8; η_U=0.82 are not the maximum, but should be typical for efficient thrusters.

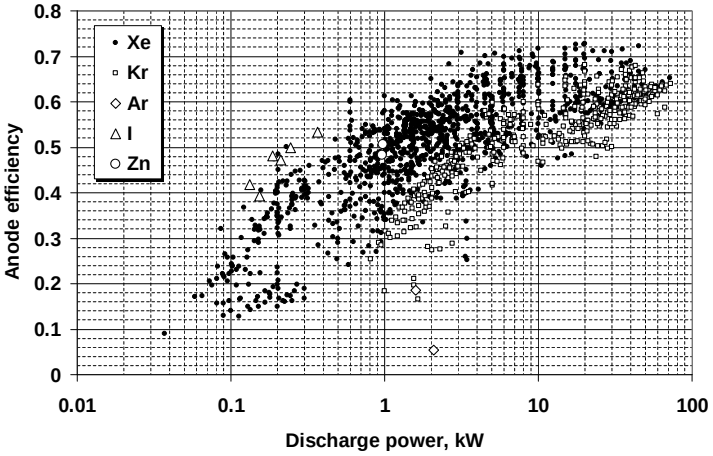

Figure 3. Anode efficiency as a function of the discharge power for a variety of HETs.

Next, consider in more detail charge and mass utilization efficiencies.

C. Accounting for Multiply Charged Ions

In our previous paper[19] it was assumed that the ratio of ion species fractions is a function of the discharge voltage. To determine the form of these functions, the data measured in the Hall thruster NASA-173Mv2[74] were used and values of η_q and γ_q were approximated by the second order polynomials. The calculated values of mass flow ions species are listed in Table 1.

Table 1 Ion species fraction, calculated using Ref. 74

Discharge voltage, V	300	400	500	600	700	800	900
μ_1 (fraction of Xe^+)	0.928	0.914	0.901	0.888	0.862	0.823	0.808
μ_2 (fraction of Xe^{2+})	0.055	0.069	0.082	0.096	0.122	0.161	0.159
μ_3 (fraction of Xe^{3+})	0.017	0.017	0.017	0.017	0.017	0.016	0.033

If to approximate the ion species fraction, listed in Table 1, by linear functions, we obtain the following approximation

$$\mu_1 = 1 - \mu_2 - \mu_3;\ \mu_2 = 1.756 \cdot 10^{-4} \cdot U_d;\ \mu_3 = 3.036 \cdot 10^{-5} \cdot U_d \tag{20}$$

where the discharge voltage U_d is expressed in volts.

In this work we have tried to collect more statistics, and used data from several thrusters tested with xenon, krypton and iodine.[37,52,55,74,75] In the cited articles different variables were used to describe the proportion of multiply charged ions. In the Refs. 37, 74, 75 the ion species number densities $\zeta_k = n_k / \sum n_k$ were measured. In this paper, we use the ion species mass flow rates which is connected with ζ_k by the expression

$$\mu_k = \left(\zeta_k \sqrt{k}\right) \Big/ \left(\sum \zeta_k \sqrt{k}\right). \tag{21}$$

In the Refs. 52, 55 the ion species currents $\Omega_k = I_k / \sum I_k$ were used, and to bring them to our variables we use the expression

$$\mu_k = \left(\Omega_k / k\right) \Big/ \sum \left(\Omega_k / k\right). \tag{22}$$

Figure 4 shows the fractions of doubly charged ions μ_2 obtained from the mentioned papers, as functions of the discharge voltage and discharge power along with the formulas of linear approximations and linear correlation coefficients. Figure 5 shows similar dependencies for triply charged ions.

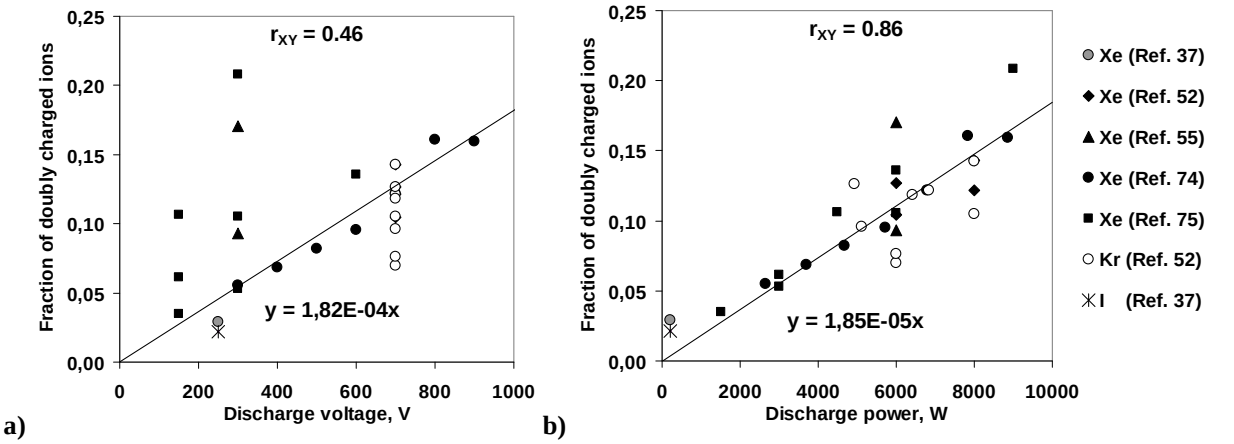

a) **b)**

Figure 4. Fraction of doubly charged ions of several HETsall effect thrusters as a function of the: a) discharge voltage; b) discharge power.

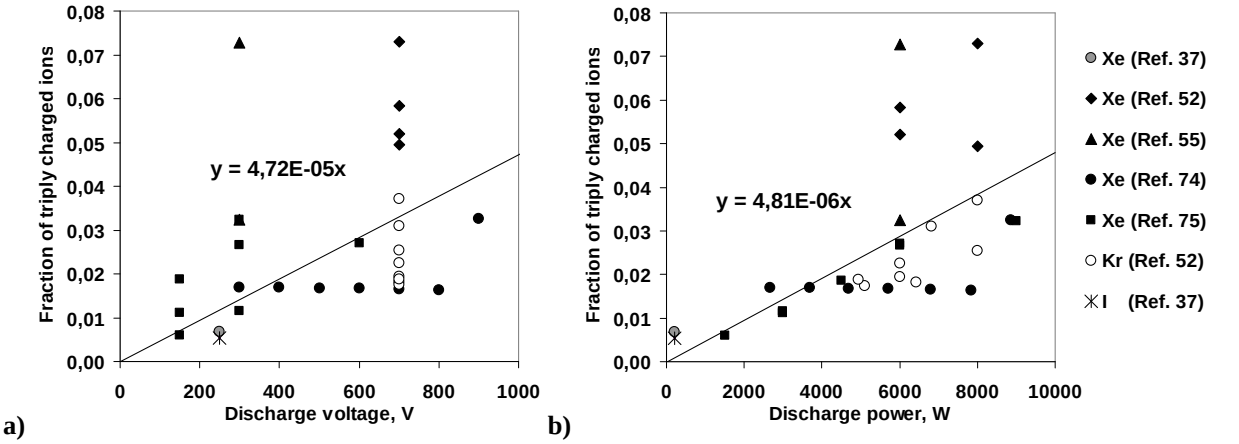

a) **b)**

Figure 5. Fraction of triply charged ions of several Hall effect thrusters as a function of the: a) discharge voltage; b) discharge power.

As can be seen, the fraction of doubly charged ions correlates better with the discharge power than discharge voltage. It is also can be noted that despite the different ionization potentials of xenon, krypton and iodine, the available data do not allow us to find difference between these dependencies for different propellants. Therefore, we can assume that the ion species fraction is a function of the discharge power. As long as there are no other data, we are also forced to assume that this function does not depend on the type of propellant.

However linear approximation presented in the Fig. 4 can not be used for high power HETs since at discharge power above 50 kW, linearly extrapolated function μ_2 is greater than one. To be able to predict the ion species fractions at very high discharge power we can assume that fraction of singly charged ions decreases not linearly but exponentially goes to zero as $\mu_1 = \exp\left(-a_1 P_d\right)$. If we consider only two ion species, then we must have $\mu_2 = 1 - \mu_1$. If we take into account three ion species, then we can assume that μ_3 exponentially approaches unity as $\mu_3 \sim 1 - \exp\left(-a_3 P_d\right)$ and therefore the fraction of doubly charged ions is $\mu_2 = 1 - \mu_1 - \mu_3$. As a result of fitting

of the presented experimental data the following two approximations could be obtained: two ion species approximation

$$\mu_1 = \exp\left(-2.33\cdot 10^{-5} P_d\right);\ \mu_2 = 1-\mu_1;\ \mu_3 = 0\,, \tag{23}$$

and three ion species approximation

$$\mu_1 = \exp\left(-2.33\cdot 10^{-5} P_d\right);\ \mu_2 = 1-\mu_1-\mu_3;\ \mu_3 = \exp\left(-4.48\cdot 10^{-6} P_d\right), \tag{24}$$

where discharge power P_d is expressed in watts.

Figure 6 shows the ion species fractions for three ion species approximation as functions of the discharge power. Figure 7 shows charge utilization efficiency calculated using Eq. (14), and correction factor γ_q calculated using Eq. (15), for the two different approximations. It is seen, that the error in prediction of the ion species fraction affects strongly on the predicted specific impulse. For example, assuming the absence of triply charged ions, the correction factor γ_q can not exceed 1.41 at any discharge power, while assuming three ion species, it will exceed 1.6 at discharge powers higher than 200 kW. The impact of the ion species fraction on the anode efficiency is not so significant.

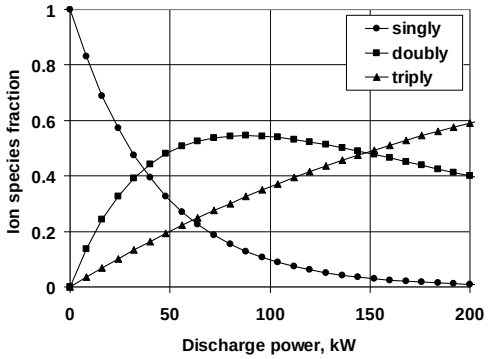

Figure 6. Extrapolation of the ion species fraction as a function of the discharge power.

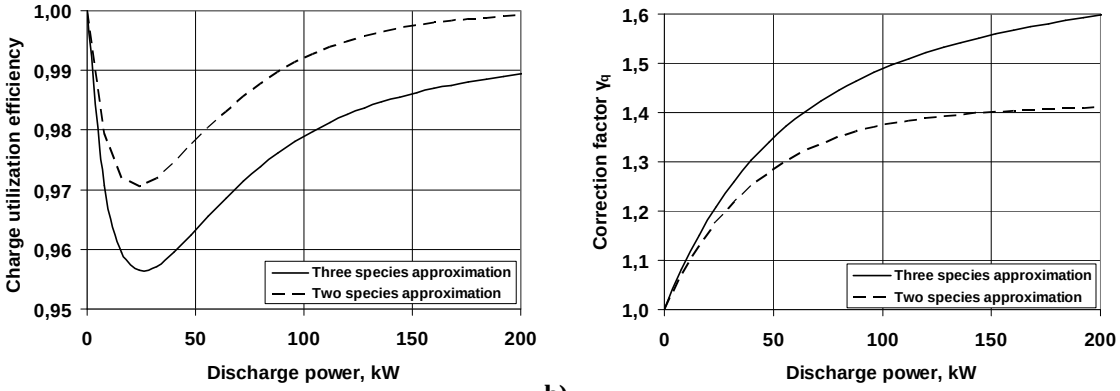

a) **b)**

Figure 7. Extrapolated performance parameters as functions of discharge power: a) η_q; b) γ_q.

If the ion species fraction actually depends on the discharge power, correct prediction of the percentage of multiply charged ions is very important for estimating the level of attainable specific impulse of high power Hall effect thrusters. Therefore, it would be good to verify, is it really the factor γ_q is a function of the discharge power, using collected database. To do this, we express the mass utilization efficiency in Eq. (18) through the other parameters, and replace the anode efficiency using Eq. (9):

$$\eta_m = \frac{T^2}{2\dot{m}_a P_d \eta_q \eta_I \eta_U}\,. \tag{25}$$

Then we express the same variable in Eq. (19) through the other parameters, and replace the anode specific impulse using Eq. (10):

$$\eta_m = \frac{T}{\dot{m}_a \gamma_q \sqrt{\eta_U}} \sqrt{\frac{M}{2eU_d}}. \tag{26}$$

Equating the expressions and replacing the variables γ_q and η_q using Eqs. (14)-(16) we obtain

$$\frac{\sum k\mu_k}{\sum \sqrt{k}\mu_k} = K_q \eta_I \sqrt{\eta_U}. \tag{27}$$

were the dimensionless parameter

$$K_q = \frac{2P_d}{T} \sqrt{\frac{M}{2eU_d}}. \tag{28}$$

is introduced. If we assume that all HETs in stable operation modes have close values of η_I, and also close values of η_U, then the parameter K_q can be used to evaluate the ion species fraction. If use two ion species approximation given by Eq. (23) and assume definite values of η_I and η_U, we can calculate from the Eq. (27) the correction factor

$$\gamma_q = \frac{2-\sqrt{2}}{1-K_q \eta_I \sqrt{\eta_U}\left(\sqrt{2}-1\right)}. \tag{29}$$

Figure 8 shows the correction factors γ_q calculated by the Eq. (29) assuming η_I = 0.8, η_U = 0.82, for a variety of HETs, as a functions of both the discharge power and discharge voltage. Symbols of chemical elements of the propellant in this figure are the same as in Figures 1 and 3. Solid line on the Fig. 8 a) shows the values of γ_q calculated by Eq. (15) assuming depending on the discharge power approximation given by Eq. (23). Solid line on the Fig. 8 b) shows values of γ_q calculated by Eq. (15) assuming depending on the discharge voltage approximation given by Eq (20).

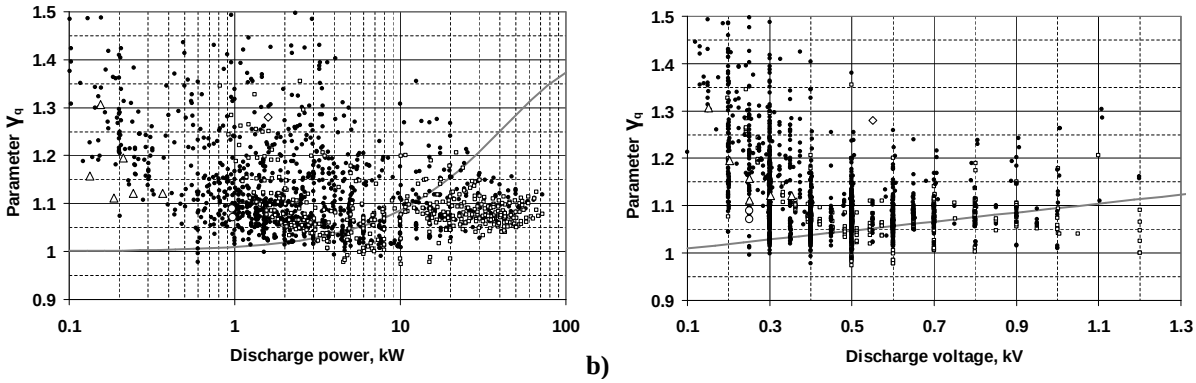

Figure 8. Estimated correction factor γ_q for different HETs at η_I=0.8, η_U=0.82: a) as a function of the discharge power; b) as a function of the discharge voltage.

At relatively low discharge power and discharge voltage the tendency of decreasing γ_q with power and voltage can be noted. Probably this is due to relatively low value of the product $\eta_I \sqrt{\eta_U}$ when HET operates insufficiently effective. If we substitute into the Eq. (29) overestimated values of η_I and η_U, we obtain the higher value of the

parameter γ_q. One can hardly speak about the correlation of the estimated experimental values of γ_q with power dependent approximation given by Eq. (23). On the other hand, at discharge voltages above 500 V there is some correlation between experimental data and voltage dependent approximation given by Eq. (20). Based on this analysis we will assume that ion species fraction is a function of the discharge voltage and will use three species approximation given by Eq. (20).

D. Mass Utilization Efficiency

In our previous studies,[48,66] it was shown that if we neglect the loss of ions on the walls, the mass utilization efficiency η_m can be estimated from the equation

$$\eta_m = 1 - \exp\left[-\left(\frac{\beta_i L \dot{m}_a}{V_a \pi D h \sqrt{2eM\Delta\varphi_I}} \right) \eta_m \right]. \tag{30}$$

Note that in the earlier experimental studies some minimum threshold of the ratio $\dot{m}_a / D$ was found below which it is not possible to achieve efficient operation.[2] The Eq. (30) clearly shows the existence of such a threshold, since it has a solution only if the expression in round brackets is greater than unity. If we use the experimental fact $L = C_L h$ we obtain the condition for the existence of solution in the form

$$\frac{C_L \beta_i}{V_a \pi \sqrt{2eM\Delta\varphi_I}} \frac{\dot{m}_a}{D} \geq 1, \tag{31}$$

which shows that at a fixed discharge voltage and fixed velocity of neutral atoms there is a clear threshold of the ratio $\dot{m}_a / D$. Experiments confirm the existence of this threshold, because at low values of this ratio Hall effect thrusters not just operates less efficiently, and usually stable operation can not be achieved at all.

In case if $\eta_I \approx const$, it is possible to express the anode mass flow rate $\dot{m}_a$ using equality:

$$\eta_m \dot{m}_a \frac{e}{M} \sum k\mu_k = I_b = \eta_I \frac{P_d}{U_d}. \tag{32}$$

Assuming scaling condition $L = C_L h$ and expressing a characteristic velocity of neutral atoms through their mass and temperature $V_a \sim \sqrt{k_B T_a / M}$ from Eqs. (16), (30) and (32) we obtain the expression for the mass utilization efficiency in the form

$$\eta_m = 1 - \exp\left[-C \frac{M \beta_i P_d}{\gamma_q' D U_d \sqrt{T_a \Delta\varphi_I}} \right], \tag{33}$$

where the factor $C = C_L \eta_I / \sqrt{2\pi^2 e^3 k_B}$ should be close in magnitude for optimized thrusters in all stable modes of operation.

Note that in the Eq. (33) there is no clear indication to the threshold of the ratio $\dot{m}_a / D$. This is because we have expressed the anode mass flow rate $\dot{m}_a$ through the discharge current, assuming the efficient mode of operation with $\eta_I \approx const$. Otherwise near the threshold the current utilization efficiency tends to zero due to the decrease of the ion current compared to discharge current. Therefore the Eq. (33) refers only to the stable and efficient enough operating modes.

The exponent in Eq. (33) indicates that use of lighter propellants instead of xenon, such as krypton or argon, should lead to a reduction of propellant utilization efficiency not only because of the lower ionization cross sections

(lower values of β_i), but also a smaller mass of their atoms. The decrease of η_m with decreasing of propellant atomic mass occurs for two reasons. First, at the same temperature the lighter atoms have higher speed and faster pass through the discharge channel, which reduces the probability of ionization. Second, at the same potential drop $\Delta\varphi_I$ the lighter ions leave the discharge channel more rapidly, which leads to a lower plasma density. Each of these factors make a contribution proportional to $\sqrt{M}$, and their combined effect leads to the fact that the exponent in the Eq. (33) is proportional to the atomic mass of the first degree.

Next, consider how the variables $\Delta\varphi_I$, T_a and β_i depend on the discharge power and voltage. After that, we can estimate the constant C in the Eq. (33) using the collected database.

There are at least two different approaches to evaluation of the characteristic potential drop in the ionization region $\Delta\varphi_I$. Some analytical studies show that this value should vary proportionally to the discharge voltage[76]. However, the experimental data,[2,77,78] show that the voltage loss ΔU is almost constant in different operation modes. If take into account that the quantities of ΔU and $\Delta\varphi_I$ are similar in magnitude,[68] we can take a typical value of $\Delta\varphi_I$ usually used in investigations of the scaling laws,[12] which is about 50 V, or we can simply include it into the sought constant in the exponent, without specifying its value.

To estimate the temperature T_a it is necessary to evaluate the thermal state of the thruster. This task is quite complex, so we will consider only the simplest approximation of constant temperature $T_a = const$. This approach can be justified by the following reasoning. The smaller size of the thruster, the higher plasma density and higher the degree of ionization. Therefore the size of the thruster tend to do as little as possible. The common limitations is thermal state of the thruster at which the materials do not lose their functional characteristics, and lifetime. Therefore, the temperature in the different optimized thrusters are usually close to each other.

The ionization reaction rate $\beta_i = \langle \sigma_i \upsilon_e \rangle$ depends on the kind of propellant and electron temperature in the ionization region. In this work these functions were numerically calculated, assuming Maxwellian electron velocity distribution function, and using the published data of ionization cross-sections for xenon,[79] krypton,[79] argon,[80] bismuth,[81] and iodine.[82] Figure 9 a) shows the obtained functions $\beta_i(T_e)$ for different types of propellant.

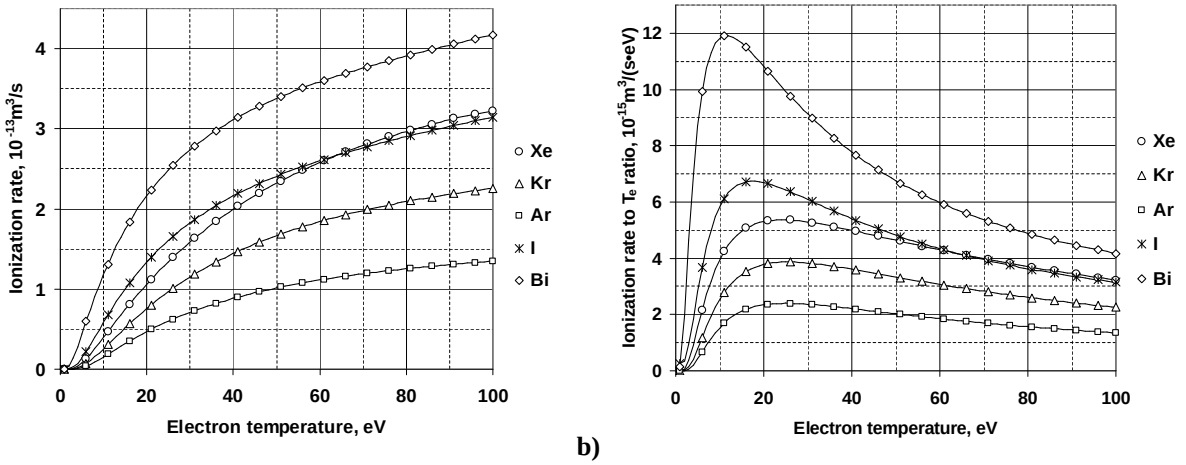

a) **b)**

Figure 9. Ionization properties of different propellants as a function of the electron temperature: a) ionization rate; b) ionization rate to electron temperature ratio.

To estimate the electron temperature in the ionization region in our previous study[19] we used the dependence $T_e \approx 0.1 \cdot U_d$, corresponding to experimental results, presented in Ref. 83. Here and below, the temperature T_e is expressed in electron volts. Similar relationship ($T_e \approx 0.12 \cdot U_d$) was obtained in Ref. 12 by generalization of several experimental studies. However, analysis of the collected database revealed that these approximations likely overestimate the electron temperature. To show this, consider Eq. (33). Provided, that $\Delta\varphi_I = const$, and assuming $T_a = const$ the mass utilization efficiency can be written as

$$\eta_m = 1 - \exp\left[-C_1 Q_1\right], \tag{34}$$

where C_1 is constant, and

$$Q_1 = \frac{M_A P_d}{D} \frac{\beta_i}{\gamma'_q U_d}, \tag{35}$$

where the relative atomic mass $M_A = M / m_u$ is introduced. At a constant discharge power, the mass utilization efficiency of a given HET should be a function of the ratio $\beta_i(T_e)/\left|\gamma'_q U_d\right|$. If electron temperature is a linear function of the discharge voltage

$$T_e = a_T U_d, \tag{36}$$

neglecting in a first approximation, the dependence of the coefficient γ'_q on the U_d, the maximum of η_m is achieved at the same electron temperature, at which the ratio $\beta_i(T_e)/T_e$ has a maximum. Figure 9 b) shows these ratios as a function of the T_e. The temperature at which mass utilization efficiency has maximum, satisfies the condition

$$T_e \frac{d\beta_i}{dT_e} - \beta_i = 0 \cdot \tag{37}$$

The solutions of the Eq. (37) obtained numerically for different propellants are listed in Table 2 in the row corresponding to the condition γ'_q =1.

Thus, if HET operates efficiently and $\eta_I \approx const$ and $\eta_U \approx const$, it is seen from the Eq. (18) that the anode to charge efficiency ratio is approximately proportional to η_m. Therefore, the ratio η_a/η_q of any effectively operating thruster should reach a maximum at the same electrons temperature in the ionization region. From Table 1 it is seen, that electron temperature, providing maximum efficiency, is close to 25 eV for all the noble gases. If, using the database, we find U_d, providing maximum of the anode efficiency, we will be able to clarify the value of the coefficient a_T in Eq. (36). Figure 10 shows the anode efficiency as a function of the discharge voltage for a number of HETs, which have been tested in a wide range of discharge voltages at close values of P_d.

Table 2 The electron temperature, providing maximum anode efficiency

	Xe	Kr	Ar	I	Bi
T_e, eV, γ'_q =1	23.9	25.3	25.1	17.5	11.6
T_e, eV, $\gamma'_q = \gamma'_q(U_d)$	20.6	22.5	22.3	15.4	10.1

It is seen that typical value of the discharge voltage, providing maximum mass utilization efficiency, is about 500 V. Therefore we can assume that value a_T=0.05 better corresponds to experimental data than previously used ratio $T_e = 0.1 \cdot U_d$. The probable reason of the difference is that previously the maximum measured temperature was used in approximation. Since the temperature drops rapidly in the ionization region because of inelastic collisions, the average temperature in the ionization region should be less.

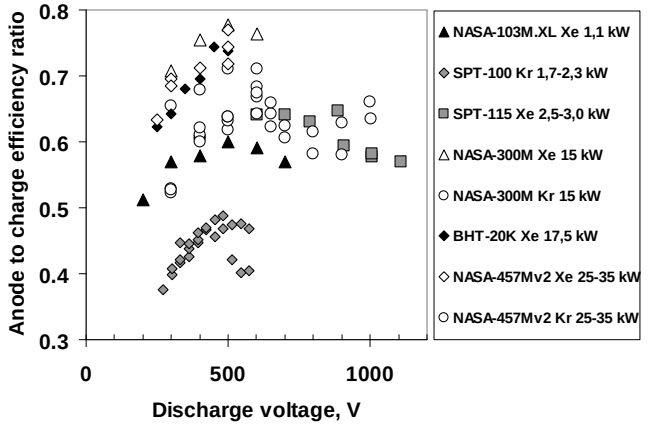

Figure 10. Anode efficiency as a function of the discharge voltage at a fixed discharge powers for several HETs

In conducted consideration we have neglected the dependence of the coefficient γ_q' on the discharge voltage. Let us consider how much it could affect the result. The factor γ_q' is defined by Eq. (16) and with taking into account the approximation of ion species fraction by Eq. (20), can be presented as a linear function of the discharge voltage

$$\gamma_q' = 1 + a_\gamma U_d , \tag{38}$$

where a_γ =2.36·10^{-4}. Using linear approximation of the electron temperature given by Eq. (36), the condition of attaining the maximal mass utilization efficiency can be written as

$$T_e\left(1+\frac{a_\gamma}{a_T}T_e\right)\frac{d\beta_i}{dT_e}-\beta_i\left[1+2\frac{a_\gamma}{a_T}T_e\right]=0\cdot \tag{39}$$

After substituting experimental data $a_T = T_e/500$, and a_γ = 2.36·10^{-4}, instead of Eq. (37) we have

$$T_e\frac{d\beta_i}{dT_e}-1.1\cdot\beta_i=0\cdot \tag{40}$$

The solutions of the Eq. (40) obtained numerically for different propellants are listed in Table 1 in the row, corresponding to the condition $\gamma_q' = \gamma_q'(U_d)$. It is seen that the revised values of optimal temperatures to about 11…13% less, than when we assume γ_q' =1. Therefore we should give the same percentage decrease to coefficient a_T, and as a result we obtain a final approximation in the form

$$T_e = 0.044\cdot U_d . \tag{41}$$

Before continuing, we note that, as it is seen in Table 2, iodine and bismuth provide maximum mass utilization efficiency at lower electron temperatures than the noble gases. From this viewpoint, they have advantages over inert gases in SPT, operating at low discharge voltages.

Now we have chosen the semiempirical approximations for all the variables in Eqs. (34),(35). We are only left to take into account in these equations the regularity of the channel diameter change with the change of discharge power:

$$D \sim \sqrt{P_d} . \tag{42}$$

Given this relationship, the expression of mass utilization efficiency takes the form

$$\eta_m = 1-\exp\left(-C_2 Q_2\right), \tag{43}$$

where

$$Q_2 = \frac{M_A\beta_i\sqrt{P_d}}{\gamma_q' U_d}, \tag{44}$$

and C_2 is the sought dimensional constant.

Figure 13 shows the anode efficiency as a function of the variable Q_2 for a variety of Hall effect thrusters. One can note that operation points relating to different thrusters and different types of propellant are grouped around the

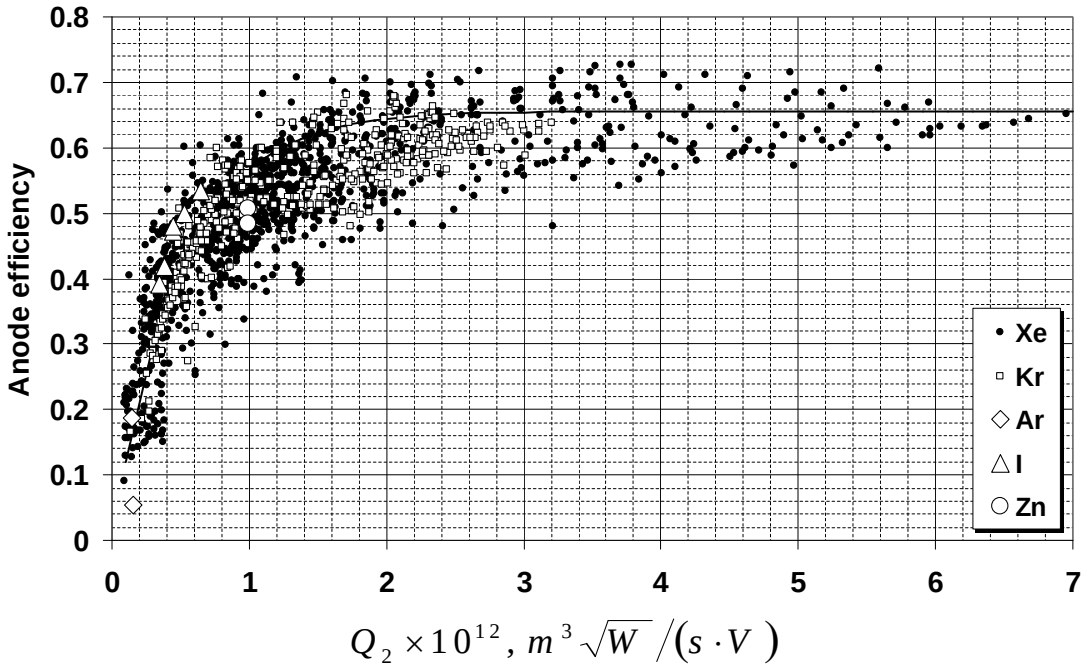

Figure 11. Anode efficiency as a function of the parameter Q_2.

same curve. To find the approximating value of the constant C_2, we use the estimate of the anode efficiency in the form

$$\eta_a = \eta_u \eta_I \eta_q \left[1 - \exp\left(-C_2 Q_2\right)\right], \tag{45}$$

where η_U = 0.82, η_I = 0.8, the factors γ_q' and η_q are calculated, using the fraction utilization efficiency, given by Eq. (20), and functions $\beta_i(T_e)$ are calculated at $T_e = 0.044 \cdot U_d$. The standard deviation of the experimental points from the approximating function given by Eq. (45) is minimal at C_2 = $2 \cdot 10^{12}$ $(V \cdot s)/\left(m^3\sqrt{W}\right)$. Solid line in Fig. 13 shows the approximating curve. The obtained value of C_2 is different from the value of $1.3 \cdot 10^{12}$, that was obtained in our previous work[19], for the following reasons: first, instead of data of four Hall effect thrusters, we used an extensive database; secondly, we refined expression of mass utilization efficiency in Eq. (33) taking into account the ion species factor γ_q' in the exponential, and thirdly, the dependence of the electron temperature on the discharge voltage has been revised.

V. Regularities of Performance

Summing up the previous section, the essence of the proposed scaling model is changing of all linear dimensions of the discharge channel in accordance with the same proportion $D \sim \sqrt{P_d}$; $h \sim \sqrt{P_d}$, and predicting the achievable output characteristics by the following procedure: set the value of η_I (in the subsequent calculations, we will assume η_I = 0.8); set the value of η_U (we will assume η_U = 0.82); calculate η_q and γ_q using a chosen model of ion species fraction (here the approximation by Eq. (20) is used); calculate the electron temperature in the ionization region (here approximation by Eq. (41) is used); calculate β_i at the obtained value of T_e; calculate η_a by Eq. (45) ; calculate I_{spa}, using Eq. (19); and calculate thrust by equation

$$T = \frac{\gamma_q}{\gamma_q'}\eta_I\sqrt{\eta_U}P_d\sqrt{\frac{2M_A m_u}{eU_d}}. \qquad (46)$$

Using obtained model it is possible to identify the main trends of the output characteristics when scaling Hall effect thrusters.

Figure 12 shows predicted anode specific impulse as a function of the discharge power at four different discharge voltages for the types of propellant considered above. At low discharge power at a given discharge voltage, the gases with higher atomic mass provide a higher specific impulse. This is due to higher mass utilization efficiency. For example, at U_d = 0.2 kV it is seen the following regularities: using xenon instead of bismuth provides a higher specific impulse only if P_d > 2 kW; the use of krypton instead of xenon increases the specific impulse if P_d > 10 kW; using argon instead of any other type of atoms, with the purpose of increasing the specific impulse, is reasonable at a discharge power exceeding 100 kW. Also it is seen that at a very low discharge voltage the use of iodine instead of xenon allows for a higher specific impulse, since with iodine, mass utilization efficiency reaches a maximum at a lower electron temperature, than with xenon, (see Fig. 9b and Table 2). Thus, for each pair of selected discharge voltage and discharge power there is some sort of propellant that provides the maximum specific impulse.

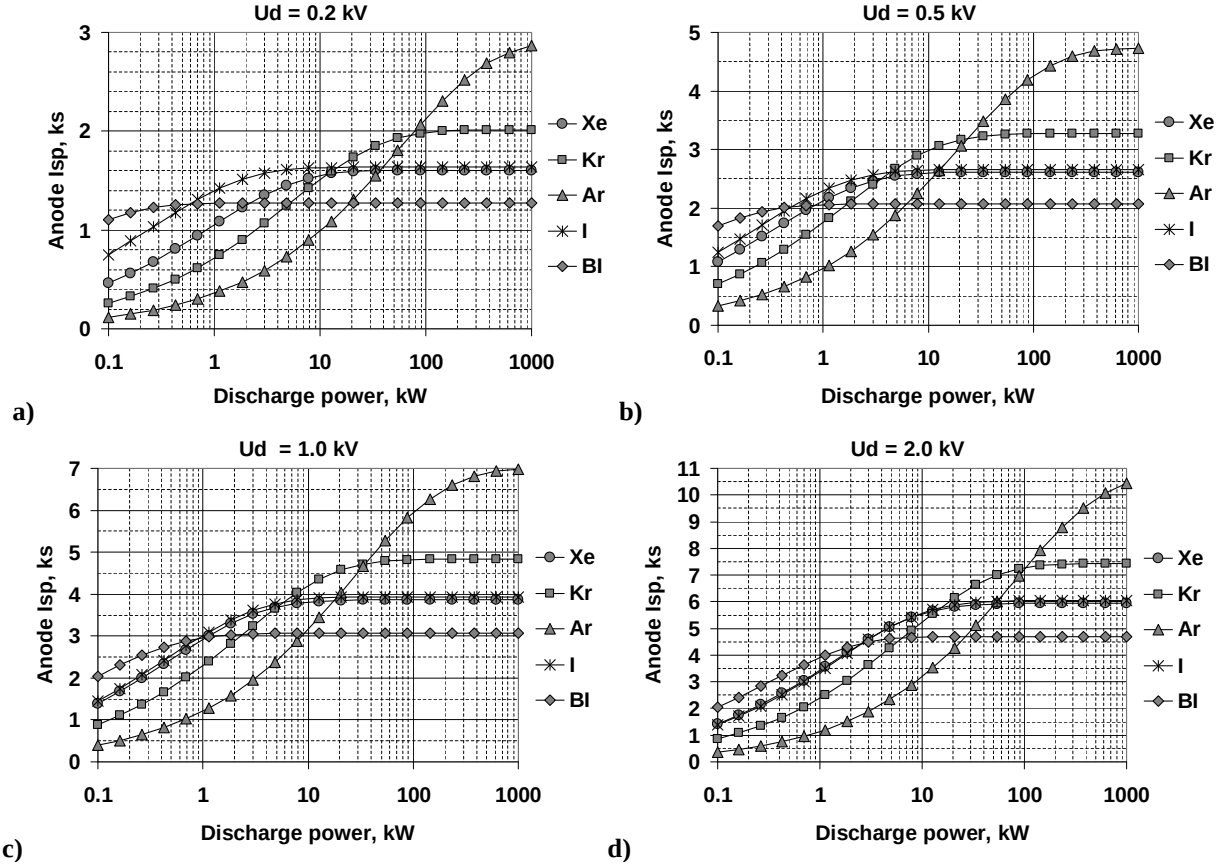

Figure 12. Predicted anode specific impulse as a function of the discharge power at different discharge voltages: a) U_d **= 0.2 kV; b)** U_d **= 0.5 kV; c)** U_d **= 1 kV; d)** U_d **= 2 kV**

Figure 13 shows predicted anode efficiency on the discharge voltage at different discharge powers for considered types of propellant. In all graphs the anode efficiency decreases with increasing the discharge voltage above 500 V. This is because in our model, the electron temperature, which ensures maximum ratio $\beta_i(T_e)/T_e$, is associated with the discharge voltage of 500 V.

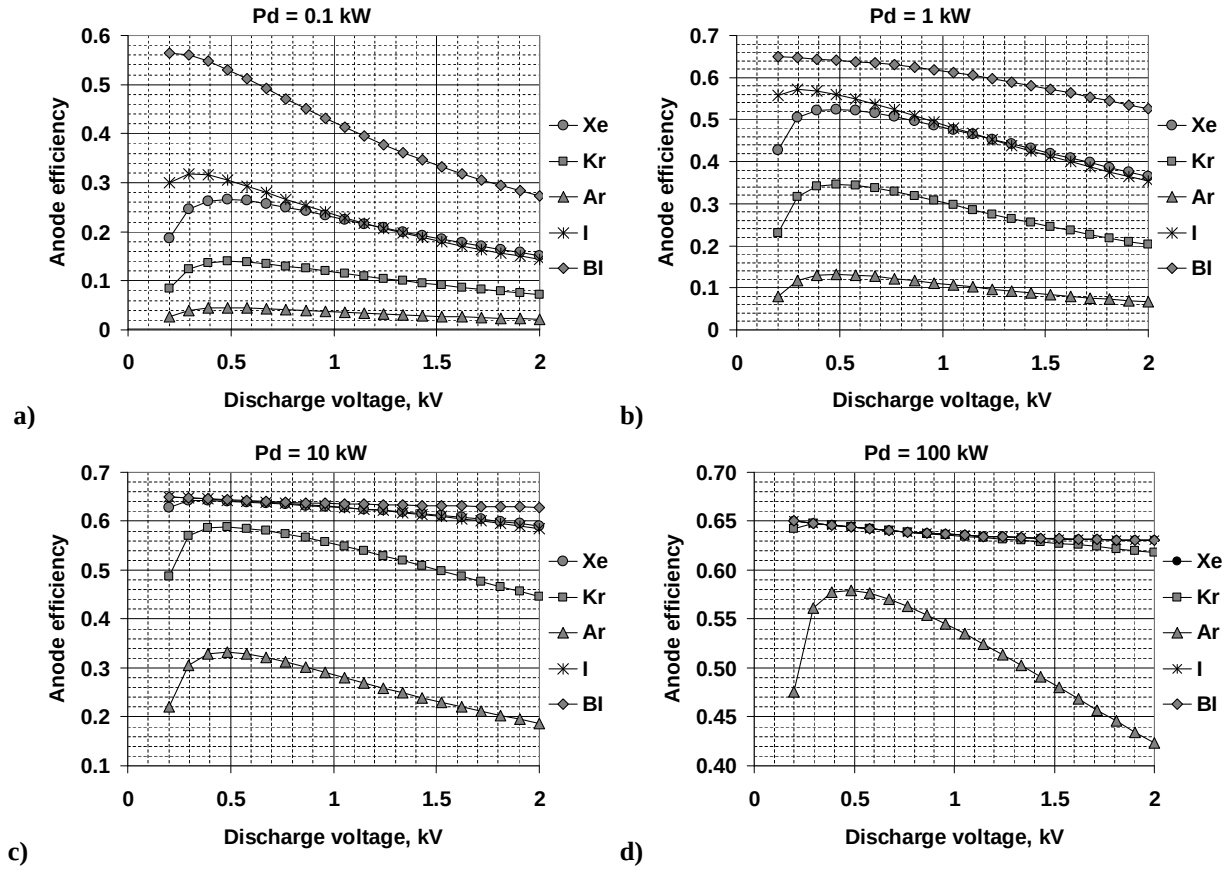

Figure 13. Predicted anode efficiency as a function of the discharge voltage at different discharge powers: a) P_d = 0.1 kW; b) P_d = 1 kW; c) P_d = 10 kV; d) P_d = 100 kW.

Bismuth provides maximum efficiency until the discharge power of the order of several kilowatts. Efficiency of iodine, which is very similar in physical characteristics to xenon, at discharge voltages less than 500 V, higher than the efficiency of xenon, and this advantage persists up to discharge power of the order of 10 kW. Efficiency of bismuth, iodine and xenon at a power of about 10 kW reach the limit values. With a power of 100 kW, efficiency with all propellants, excluding argon, is about the same. It can also be noted, that with the increasing discharge power of the rate of decline in efficiency, when increasing the discharge voltage, decreases.

Figures 14-17 shows the universal diagrams of thrust performance, calculated using the presented model for xenon, krypton, argon and bismuth respectively. The diagram for iodine is not presented because it is very similar to the diagram of xenon. Diagrams show the anode specific impulse as a function of thrust. Two sets of curves are shown in the diagrams. One set corresponds to a change of the discharge voltage for different values of fixed discharge power. The discharged power values are shown near the beginning of each curve. Another set of curves corresponds to change of discharge power at different fixed values of the discharge voltage. The discharge voltage values are shown near the end of each curve. Diagrams are useful in that they allow fast, at the given values of thrust and anode specific impulse to determine at what power level and the discharge voltage one can achieve the desired parameters. Conversely, by specifying the intersection point of the curves with predetermined discharge power and discharge voltage one can estimate the expected thrust and the anode specific impulse. Similar diagrams in which one of the axes postponed anode specific impulse, together with those shown in Figures 14-17, allow to define a complete set of parameters characterizing the performance of Hall effect thruster.

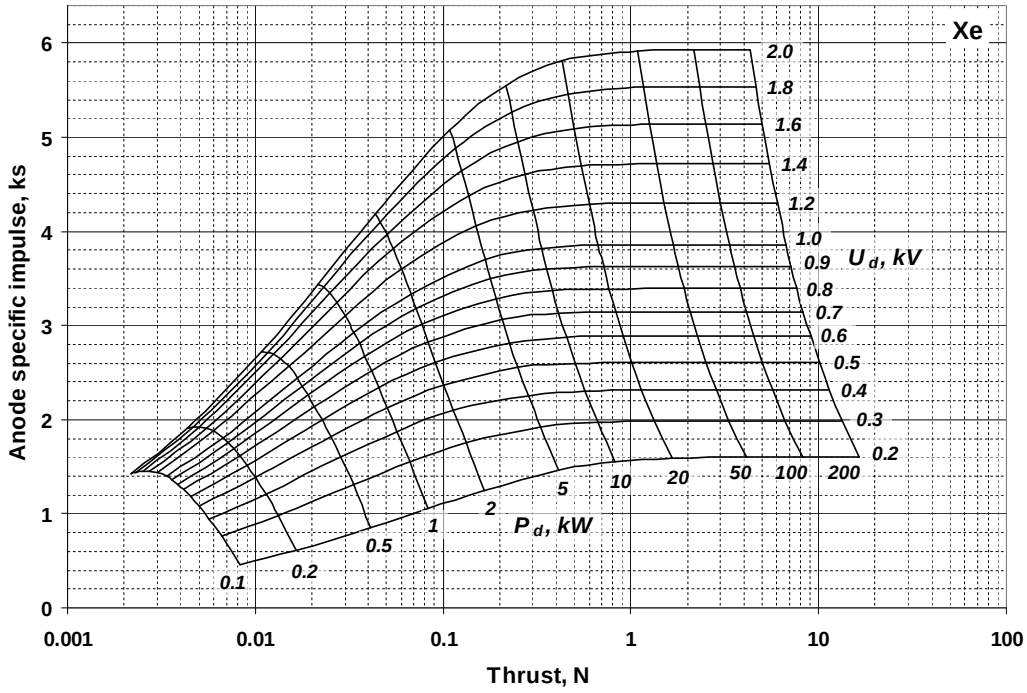

Figure 14. Predicted anode specific impulse as a function of the thrust of Xe at different discharge powers and discharge voltages

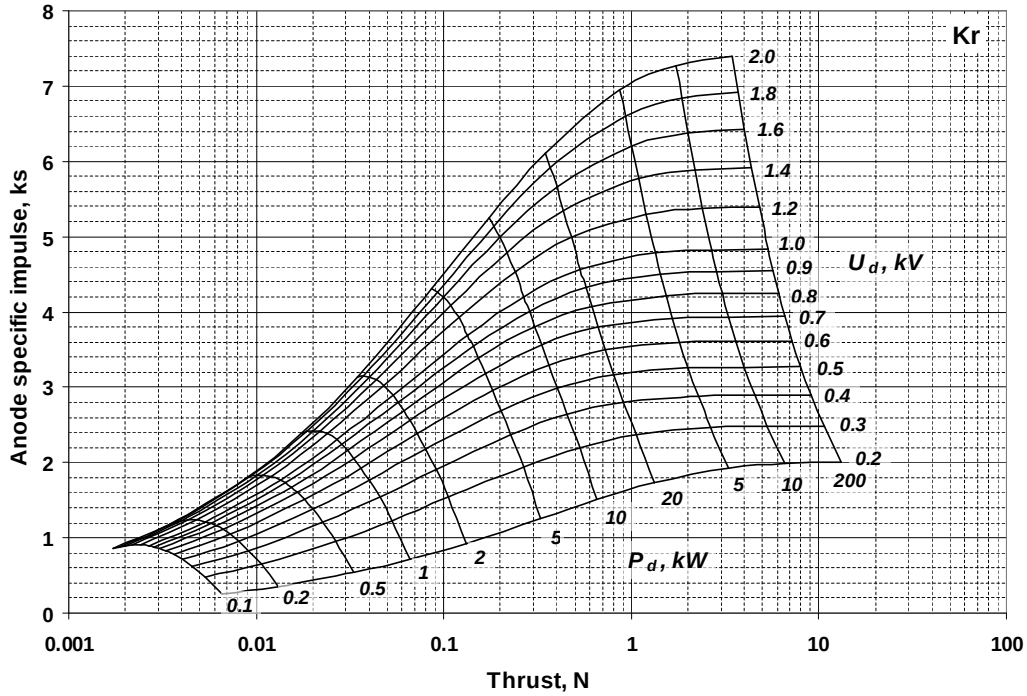

Figure 15. Predicted anode specific impulse as a function of the thrust of Kr at different discharge powers and discharge voltages

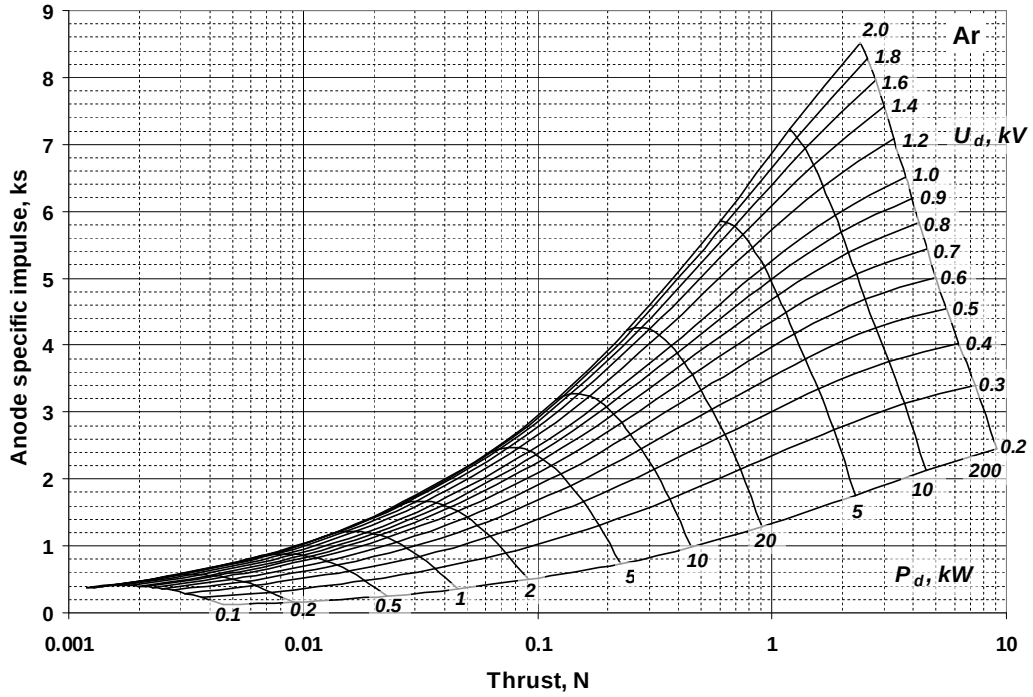

Figure 16. Predicted anode specific impulse as a function of the thrust of Ar at different discharge powers and discharge voltages

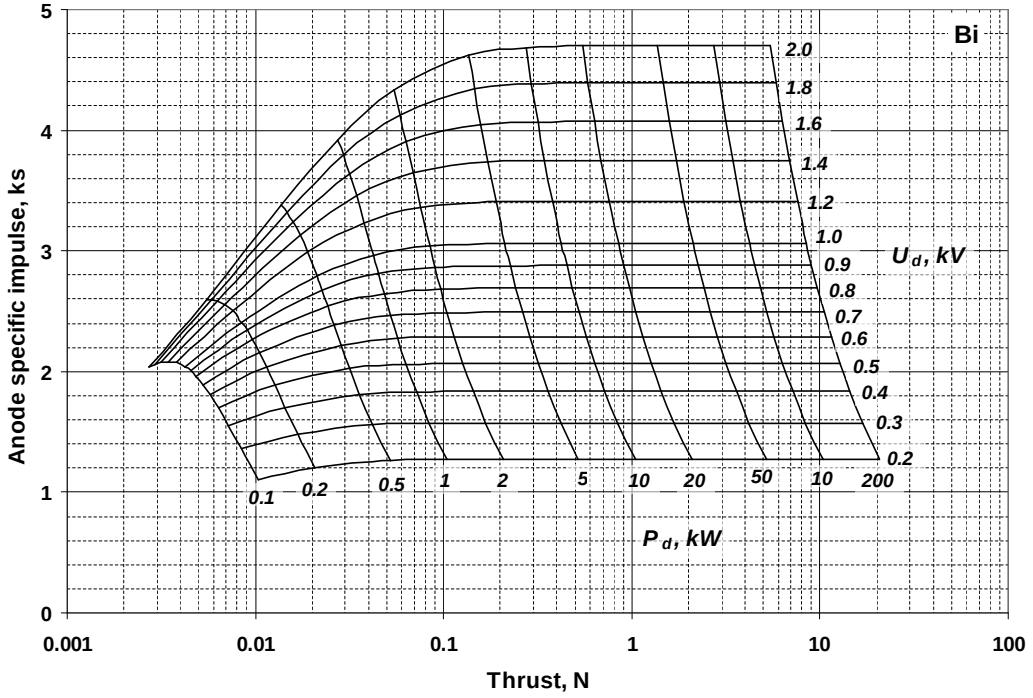

Figure 17. Predicted anode specific impulse as a function of the thrust of Bi at different discharge powers and discharge voltages.

VI. Conclusion

In this study, we examined the problem of scaling Hall effect thrusters and made an attempt to justify the following two points. First, when scaling, linear dimensions of the discharge channel can not be considered as independent variables. Unless come into conflict with experimental data, the model must accept two terms of scaling: $L \approx h$ and $h \sim D$. Secondly, the provision of physical similarity, when scaling is hardly feasible, if only we do not want to simulate work of the thruster in laboratory conditions, using forced cooling.

It is shown that strict similarity of plasma parameters is possible only at invariance of at least two dimensionless criteria. $K_B = \left(eh^2 B_0^2\right) / \left(mU_d\right)$ and $K_m = \left(\dot{m}_a \sigma_{im}\right) / \left(\pi D M V_a\right)$, in geometrically similar thrusters, at the same type of propellant, and at the same discharge voltage.

When scaling, it is necessary to ensure the condition of the limited heat flow on the channel walls by the condition $D \sim \sqrt{P_d}$, then change all the dimensions in the same proportion and estimate the performance characteristics of the scaled thruster. The approach is based on the obtained semi-empirical expressions, describing different coefficients in the phenomenological performance model as functions of operation conditions. Empirical coefficients of the model are found using an extensive database containing published test results of many Hall effect thrusters. The most extensively studied the behavior of mass utilization efficiency and charge utilization efficiency. The prospects for further development of the model are related to the investigation of behavior regularities of current utilization efficiency, as well as losses associated with the ion velocity distribution function. Also beyond the scope of the study, there were questions about the magnitude of the magnetic field and the features of the optimization of its configuration under various operating conditions. Successful investigation of these problems can provide substantial progress in creation of the complete methodology of scaling Hall effect thrusters.

References

[1]Morozov, A. I., and Melikov, I.V., "On the Similarity of the Processes in Plasma Accelerators with Closed Electron Drift (ACDE) in the Presence of Ionization," *Journal of Technical Physics*, Vol. 64, No. 3, 1974, pp. 544–548 (in Russian).

[2]Bugrova, A. I., Maslennikov, N. A., and Morozov, A. I., "Similarity Laws of the ACDE Integral Characteristics," *Journal of Technical Physics*, Vol. 61, No. 6, 1991, pp. 45–51 (in Russian).

[3]Khayms, V., and Martinez-Sanchez, M., "Design of a miniaturized Hall thruster for microsatellites", *Proceedings of the 32nd AIAA/ASME/SAE/ASEE Joint Propulsion Conference & Exhibit*, No. AIAA-96-3291, FL, July 1996.

[4]Kim, V., Kozlov, V., Skrylnikov A., et al., "Development and Investigation of the SPT-20 and SPT-25 Laboratory Models", *Proceedings of the 1st Annual International Conference and Exhibition. Small Satellites: New technologies, achievements, problems and prospects for the International co-operation in the new millenium*, section YIII "Jet Propulion", Moscow, 2000.

[5]Ahedo, E. and Gallardo, J., "Scaling Down Hall Thrusters," *Proceedings of the 28th International Electric Propulsion Conference*, No 2003-104, Toulouse, France, March 2003.

[6]Andrenucci, M., Biagioni, L., Marcuccio, S., Paganucci, F., and Tobak, M., "Fundamental Scaling Laws for Electric Propulsion Concepts. Part 1: Hall Effect Thrusters," *Proceedings of the 28th International Electric Propulsion Conference*, No. 2003-259, Toulouse, France, March 2003.

[7]Battista, F., Marco, E. A. D. and Misuri, T., "A Review of the Hall Thruster Scaling Methodology," *Proceedings of the 30th International Electric Propulsion Conference*, Paper 2007-313, Florence, Italy, Sept. 2007.

[8]Misuri, T., Battista, F., Barbieri, C., De Marco, E. A., Andrenucci, M., "High Power Hall Thrusters Design Options," *Proceedings of the 30th International Electric Propulsion Conference*, Paper 2007-311, Sept. 2007.

[7]Ashkenazy, J., Shitrit, S., and Appelbaum, G., "Hall Thruster Modifications for Reduced Power Operation, " *Proceedings of the 29th International Electric Propulsion Conference*, No. 2005-080, Princeton, NJ, Oct.–Nov. 2005.

[8]Dannenmayer, K., and Mazouffre, S., "Sizing of Hall effect thrusters with input power and thrust level: An Empirical Approach," *J.Tech. Phys*., 49, 3–4, 231–254, 2008.

[9]Kim, V., "Main Physical Features and Processes Determining the Performance of Stationary Plasma Thrusters," *Journal of Propulsion and Power*, Vol. 14, No. 5, 1998, pp. 736–743.

[10]Choueiri E. "An Overview of Plasma Oscillations in Hall Thrusters," *Physics of Plasmas*, 8(4):1411-1426, 2001.

[11]Gorshkov, O., Shagayda, A., and Irishkov, V., "The Influence of the Magnetic Field Topology on Hall Thruster Performance", *Proceedings of the 42nd AIAA/ASME/SAE/ASEE Joint Propulsion Conference & Exhibit*, No. AIAA 2006-4472, Sacramento, California, July 2006.

[12]Dannenmayer, K., and Mazouffre, S., "Elementary Scaling Relations for Hall Effect Thrusters," *Journal of Propulsion and Power*, Vol. 27, No. 1, 2011, pp. 236-245.

[13]Bober, A. S., and Maslennikov, N. A., "SPT in Russia—new achievements", *Proceedings of the 24th International Electric Propulsion Conference*, No. IEPC-95-06, Moscow, 1995.

[14]Gorshkov, O., Shagayda, A., and Muravlev, V., "The Experience of Hall Thruster Research and Development". *Proceedings of the 57th IAC/IAF/IAA (International Astronautical Congress)*, No. IAC-06-C4.4.08, Valencia, Spain, Oct. 2-6 2006.

[15]Blinov, N., Gorshkov, O., and Shagayda, A., "Experimental investigation of magnetic field topology influence on structure of acceleration layer and performance of Hall thrusters", *Proceedings of the 29th International Electric Propulsion Conference*, No. IEPC-2005-033, Princeton (USA), October 30 - November 04, 2005.

[16]Gorshkov, O. A. and Shagayda, A. A., "The Criterion of Optimal Configuration of Magnetic Field in a Thruster with Closed Electron Drift, " *High Temperature*, 2008, Vol. 46, No. 4, pp. 529–534.

[17]Loyan A. V., Maksymenko T.A. "Performance Investigation of SPT-20M Low Power Hall Effect Thruster", *Proceedings of the 30th International Electric Propulsion Conference*, No. IEPC-2007-100, Florence, Italy, September 2007.

[18]Maslennikov, N. A., "Lifetime of the Stationary Plasma Thruster," *Proceedings of the 24th International Electric Propulsion Conference*, No. IEPC-95-75, Moscow, 1995.

[19]Shagayda, A. A., and Gorshkov, O. A., "Hall-Thruster Scaling Laws", *Journal of Propulsion and Power*, Vol. 29, No. 2, 2013, pp. 466-474.

[20]Sankovic, J. M., Hamley, J. A., Haag, T. W., "Performance Evaluation of the Russian SPT-100 Thruster at NASA LeRC," *Proceedings of the 23rd International Electric Propulsion Conference*, No. 93-094, September 1993.

[21]Arkhipov, B., Kim, V., Kozlov, V., Koryakin, A., Murashko, V., Nesterenko, A., Skrylnikov, A., Lawrence, T., "Small SPT Unit Development and Tests," *Proceedings of the 3rd International Conference on Spacecraft Propulsion*, Cannes, France, October 2000.

[22]Jacobson, D. T., Jankovsky, R. S., "Test results of a 200W class Hall thruster", *Proceedings of the* 34th *AIAA/ASME/SAE/ASEE Joint Propulsion Conference & Exhibit*, No. AIAA-98-3792, Cleveland, Ohio, VA, 1998.

[23]Manzella, D.H., Oleson, S., Sankovic, J., Haag, Ò., Semenkin, A., Kim, V., "Evaluation of Low Power Hall Thruster Propulsion,", *Proceedings of the 32nd AIAA/ASME/SAE/ASEE Joint Propulsion Conference & Exhibit*, No. AIAA-96-2736, FL, July 1996.

[24]Kim V., Kozlov V., Popov G., Skrylnikov A., "Plasma Parameter Distribution Determination in SPT-70 plume," *Proceedings of the 28th International Electric Propulsion Conference*, No. IEPC-2003-107, Toulouse, March 2003.

[25]Arkhipov, B., Koryakin, A., Murashko, V., Nesterenko, A., Khoromsky, I., Kim, V., Kozlov, V., Popov, G., and Skrylnikov, A., "The Results of Testing and Effectiveness of Kr-Xe Mixture Application in SPT," *Proceedings of the 27th International Electric Propulsion Conference*, No. IEPC-01-064, Pasadena, CA, October, 2001.

[26]Kim, V., Popov, G., Kozlov, V., Skrylnikov, A., and Grdlichko, D., "Investigation of SPT Performance and Particularities of its Operation with Kr/Xe Mixtures", *Proceedings of the 27th International Electric Propulsion Conference*, No. IEPC-01-065, Pasadena, CA, October, 2001.

[27]Nakles, M. R., Hargus, W. A., Delgado, J. J., and Corey, R. L., "A comparison of xenon and krypton propellant on an SPT-100 Hall thruster," *Proceedings of the 32nd International Electric Propulsion Conference*, No. IEPC-2011-003, Wiesbaden, Germany, September 2011.

[28]Bouchoule A., Lazurenko, A., Vial, V., Kim V., Kozlov V., and Skrylnikov, A., "Investigation of the SPT Operation Particularities Under High Discharge Voltages," *Proceedings of the 28th International Electric Propulsion Conference*, No. IEPC-2003-211, Toulouse, France, March 2003.

[29]Manzella D., Sarmiento C., Sankovic J., Haag T., "Performance Evaluation of the SPT-140," *Proceedings of the 25th International Electric Propulsion Conference*, No. IEPC-97-059, Cleveland, OH, August 1997.

[30]Murashko, V., Koryakin, A., Nyatin, A., Kim, V., Popov, G., Romashko., A., et al., "State of the art and prospects of electric propulsion in Russia," *Proceedings of the 28th International Electric Propulsion Conference*, No. IEPC-2003-340, Toulouse, France, March 2003.

[31]Marchandise, F., Cornu, N., Arcis, N., and Arrat, D., "Compact Hall Effect Assembly Propulsion subsystem PPS®X00, first test results in the range 300W-500W," *Proceedings of the 32nd International Electric Propulsion Conference*, No. IEPC-2011-111, Wiesbaden, Germany, September 2011.

[32]Albarède, L., Bouchoule, A., Lazurenko, A., Kim, V., Kozlov, V., and Skrylnikov, A., "Characteristics of PPS-1350 type thrusters under increased discharge voltages and comparison with hybrid codes simulation results," *Proceedings of the* 29th *International Electric Propulsion Conference*, No. IEPC-2005-136, Princeton University, October – November 2005.

[33]Vial, V., Godard, L., Cornu, N., Coulaud, E., and Arrat, D., "PPS®1350-G Performance assessment with permanent magnets," *Proceedings of the 32nd International Electric Propulsion Conference*, No. IEPC-2011-119, Wiesbaden, Germany, September 2011.

[34]Duchemin, O., Dumazert, P., Clark, S. D., and Mundy, D.H., "Development and Testing of a High-Power Hall Thruster," *Proceedings of the 28th International Electric Propulsion Conference*, No. IEPC-2003-032, Toulouse, France, March 2003.

[35]Biagioni, L., Saverdi, M., Berti, M., Cesari, U., and Andrenucci, M., "Design and Preliminary Characterization of a 5 Kw Hall Thruster Prototype," *Proceedings of the 28th International Electric Propulsion Conference*, No. IEPC-2003-228, Toulouse, France, March 2003.

[36]Hruby, V., Monheiser, J., Pote, B., Freeman, C., and Connolly, W., "Low Power, Hall Thruster Propulsion System," *Proceedings of the 26th International Electric Propulsion Conference*, No. IEPC-1999-092, Kitakyushu, Japan, October 1999.

[37]Szabo, J., Pote, B., Paintal, S., Robin, M., Hillier, A. I., Branam, R. D. and Huffman, R. E., "Performance Evaluation of an Iodine-Vapor Hall Thruster," *Journal of Propulsion and Power*, Vol. 28, No. 4, July–August 2012, pp. 848-857.

[38]Lobbia, R. B., and Gallimore, A. D. "Performance Measurements from a Cluster of Four Hall Thrusters," *Proceedings of the 30th International Electric Propulsion Conference*, No. IEPC-2007-177, Florence, Italy, September 2007.

[39]Nakles, M. R., Barryy, R. R., Larson, C. W., and Hargus, W. A., "A Plume Comparison of Xenon and Krypton Propellant on a 600 W Hall Thruster," *Proceedings of the 31st International Electric Propulsion Conference,* No. IEPC-2009-115, Ann Arbor, Michigan, USA, September 2009.

[40]Pote, B., and Tedrake, R., "Performance of a High Specific Impulse Hall Thruster," *Proceedings of the 27th International Electric Propulsion Conference*, No. IEPC-2001-035, Pasadena, CA, October 2001.

[41]Szabo, J. J., and Azziz, Y., "Characterization of a High Specific Impulse Xenon Hall Effect Thruster," *Proceedings of the* 29th *International Electric Propulsion Conference*, No. IEPC-2005-324, Princeton University, October – November 2005.

[42]Szabo, J., Robin, M., Duggan, J., and Hofer, R.R., "Light Metal Propellant Hall Thrusters," *Proceedings of the 31st International Electric Propulsion Conference*, No. IEPC-2009-138, Ann Arbor, Michigan, USA, September 2009.

[43]de Grys, K., Meckel, N., Callis, G., Greisen, D., Hoskins, A., King, D., et al., "Development and Testing of a 4500 Watt Flight Type Hall Thruster and Cathode," *Proceedings of the 27th International Electric Propulsion Conference*, No. IEPC-2001-011, Pasadena, CA, October 2001.

[44]Fisher, J., Wilson, A., King, D., Meyer, S., de Grys, K., Werthman, L., "The Development and Qualification of a 4.5 kW Hall Thruster Propulsion System for GEO Satellite Applications," *Proceedings of the 28th International Electric Propulsion Conference*, No. IEPC-2003-295, Toulouse, France, March 2003.

[45]Hofer, R. R., Mikellides, I. G., Katz, I., and Goebel, D. M., "BPT-4000 Hall Thruster Discharge Chamber Erosion Model Comparison with Qualification Life Test Data," *Proceedings of the 30th International Electric Propulsion Conference*, No. IEPC-2007-267, Florence, Italy, September 2007.

[46]Pote, B., Hruby, V., Monheiser, J., "Performance of an 8 kW Hall Thruster," *Proceedings of the 26th International Electric Propulsion Conference*, No. IEPC-1999-080, Kitakyushu, Japan, October 1999.

[47]Szabo, J., Pote, B., Hruby, V., Byrne, L., Tedrake, R., Kolencik, G., Kamhawi, H., Haag, T. W., "A Commercial One Newton Hall Effect Thruster for High Power In-Space Missions," *Proceedings of the 47th AIAA/ASME/SAE/ASEE Joint Propulsion Conference& Exhibit*, No. AIAA-2011-6152, San Diego, CA, July – August 2011.

[48]Peterson, P., Kamhawi, H., Manzella, D., and Jacobson, D., "Hall Thruster Technology for NASA Science Missions: HiVHAc Status Update," *Proceedings of the 43rd AIAA/ASME/SAE/ASEE Joint Propulsion Conference & Exhibit*, No. AIAA-2007-5236, Cincinnati, OH, July 2007.

[49]Manzella, D., and Jacobson, D., "Investigation of Low-Voltage/High-Thrust Hall Thruster Operation," *Proceedings of the 39th AIAA/ASME/SAE/ASEE Joint Propulsion Conference & Exhibit*, No. AIAA-2003-5004, Huntsville, Alabama, July 2003.

[50]Huang, W., Kamhawi, H., and Shastry, R., "Farfield Ion Current Density Measurements before and after the NASA HiVHAc EDU2 Vibration Test," *Proceedings of the 48th AIAA/ASME/SAE/ASEE Joint Propulsion Conference & Exhibit*, No. AIAA-2012-4195, Atlanta, GA, July –August 2012.

[51]Kamhawi, H., Manzella, D., Pinero, L., Haag, T., and Mathers, A., "Preliminary Performance Characterization of the High Voltage Hall Accelerator Engineering Model Thruster," *Proceedings of the 31st International Electric Propulsion Conference,* No. IEPC-2009-093, Ann Arbor, Michigan, USA, September 2009.

[52]Linnell, J. A., "An Evaluation of Krypton Propellant in Hall Thrusters," *Ph.D. Dissertation*, Aerospace Engineering Dept., The University of Michigan, 2007.

[53]Hofer, R. R., Peterson, P. Y., Gallimore, A. D., and Jankovsky, R. S., "A High Specific Impulse Two-Stage Hall Thruster with Plasma Lens Focusing," *Proceedings of the 27th International Electric Propulsion Conference*, No. IEPC-2001-036, Pasadena, CA, October 2001.

[54]Hofer, R. R. and Jankovsky, R. S., "The influence of current density and magnetic field topography in optimizing the performance, divergence, and plasma oscillations of high specific impulse Hall thrusters," *Proceedings of the 28th International Electric Propulsion Conference*, No. IEPC-2003-142, Toulouse, France, March 2003.

[55]Hofer, R. R., Goebel, D. M., Mikellides, I, G., Katz, I., "Design of a Laboratory Hall Thruster with magnetically Shielded Channel Walls, Phase II Experiments: Experiments," *Proceedings of the 48th AIAA/ASME/SAE/ASEE Joint Propulsion Conference & Exhibit*, No. AIAA-2012-3788, Atlanta, GA, July –August 2012.

[56]Mason, L., Jankovsky, R., Manzella, D., "1000 Hours of Testing on a 10 Kilowatt Hall Effect Thruster," *Proceedings of the 37th Joint. Propulsion Conference & Exhibit*, No. AIAA-2001-3773, Salt Lake City, UT, July 2001.

[57]Kamhawi, H., Haag, T. W., Jacobson, D. T., and Manzella, D. H., "Performance Evaluation of the NASA-300M 20 kW Hall Effect Thruster," *Proceedings of the 47th AIAA/ASME/SAE/ASEE Joint Propulsion Conference& Exhibit*, No. AIAA-2011-5521, San Diego, CA, July – August 2011.

[58]Peterson, P., Jacobson, D., Manzella, D., John, J.W., "The Performance and Wear Characterization of a High-Power High-Isp NASA Hall Thruster," *Proceedings of the 41st AIAA/ASME/SAE/ASEE Joint Propulsion Conference& Exhibit*, No. AIAA-2005-4243, Tucson, AZ, July 2005.

[59]Manzella, D.H., Jankovsky R.S., Hofer, R.R, "Laboratory Model 50kW Hall Thruster," *Proceedings of the 38th AIAA/ASME/SAE/ASEE Joint Propulsion Conference& Exhibit*, No. AIAA-2002-3676, Indianapolis, Indiana, July 2002.

[60]Jacobson, D., and Manzella, D., "50 kW Class Krypton Hall Thruster Performance," *Proceedings of the 39th AIAA/ASME/SAE/ASEE Joint Propulsion Conference & Exhibit*, No. AIAA-2003-4550, Huntsville, Alabama, July 2003.

[61]Soulas, G. C., Haag, T. W., Herman, D. A., Huang, W., Kamhawi, H., and Shastry, R., "Performance Test Results of the NASA-457M v2 Hall Thruster," *Proceedings of the 48th AIAA/ASME/SAE/ASEE Joint Propulsion Conference & Exhibit*, No. AIAA-2012-3940, Atlanta, Georgia, July – August 2012.

[62]Ozaki, T., Inanaga, Y., Nakagawa, T., and Osuga, H., "Development Status of 200mN Class Xenon Hall Thruster of MELCO," *Proceedings of the* 29th *International Electric Propulsion Conference*, No. IEPC-2005-064, Princeton University, October – November 2005.

[63]Dignani, D., Ducci, C., Cifali, G., Rossetti, P., and Andrenucci, M., "HT-100 Hall thruster characterization tests results", *Proceedings of the 32nd International Electric Propulsion Conference*, No. IEPC-2011-191, Wiesbaden, Germany, September 2011.

[48]Belikov, M., Gorshkov, O., Dyshlyuk, E., Lovtzov, A., and Shagayda, A., "Development of Low-Power Hall Thruster with Lifetime up to 3000 Hours," *Proceedings of the 30th International Electric Propulsion Conference*, No. IEPC-2007-129, Florence, Italy, September 2007.

[64]Gorshkov, O. A., Belikov, M. B., Muravlev V. A., Shagayda A. A., Shanbhogue, K. M., Premkumar, S., Nandalan, V., and Jayaraman M., "The GSAT-4 Electrical Propulsion Subsystem Based on the KM-45 HET," *Proceedings of the 58th International Astronautical Congress*, No. IAC-07-C4.4.01, India, Hyderabad, 2007.

[65]Gorshkov, O., Shagayda, A., Muravlev, V., "The Experience of Hall Thruster Research and Development," *Proceedings of the 57th International Astronautical Congress*, No. IAC-06-C4.4.08, Valencia, Spain, October 2006.

[66]Shagayda, A. A., Gorshkov, O. A. and Tomilin, D. A., "Influence of the erosion of the discharge channel wall on the efficiency of a stationary plasma thruster," *Technical Physics*, 2012, Vol. 57, No. 8, pp. 1083-1089.

[67]Ding, Y. J.; Yu, D. R.; Li, H.; Ning, Z. X.; Jia, D. C., "Study on Similarity Criteria of Hall Effect Thrusters," *Contributions to Plasma Physics*, vol. 49, issue 6, pp. 362-372

[68]Bugrova, A. I., Lipatov, A. S., Morozov, A. I., and Churbanov, D. V. "On a similarity criterion for plasma accelerators of the stationary plasma thruster type," *Technical Physics Letters*, Vol. 28, No. 10, 2002, pp. 821-823.

[69]Inan, U. S., Gokowski, M., *Principles of Plasma Physics for Engineers and Scientists*, Cambridge University Press, 2011, pp. 246-248.

[70]Erofeev, V. S., and Zharinov, A. V., ''Ion Acceleration in the EH Sheath with Closed Hall Current,'' *Plasma accelerators*, Mashinostroenie, Moscow, 1972, pp. 65– 67 (in Russian).

[71]Brown, D. L., Larson, C. W., Beal, B. E., and Gallimore, A. D. "Methodology and Historical Perspective of a Hall Thruster Efficiency Analysis," *Journal of Propulsion and Power*, Vol. 25, No. 6, 2009, pp. 1163-1177.

[72]Gorshkov, O. A., and Shagayda, A. A., "Determining the Efficiency of a Plasma Thruster with Closed Electron Drift," *Technical Physics Letters*, Vol. 34, No. 2, 2008, pp. 153–155.

[73]Gorshkov, O., Blinov, N., Rizakhanov, R., Shagayda, A., "Hall Effect Thruster with high Specific Impulse", *Proceedings of the 4th International Spacecraft Propulsion Conference*, Sardinia, Italy, 2-9 June 2004.

[74]Hofer, R. R., and Gallimore, A. D., "Ion Species Fractions in the Far-Field Plume of a High-Specific Impulse Hall Thruster," *Proceedings of the 39th AIAA/ASME/SAE/ASEE Joint Propulsion Conference & Exhibit*, No. AIAA-2003-5001, Huntsville, Alabama, July 2003.

[75]Reid, B. M., Shastry, R., Gallimore, A. D. and Hofer, R. R., "Angularly-Resolved E×B Probe Spectra in the Plume of a 6-kW Hall Thruster", *Proceedings of the 44th AIAA/ASME/SAE/ASEE Joint Propulsion Conference & Exhibit*, No. AIAA 2008-5287,, Hartford, CT, 21 - 23 July 2008.

[76]Cohen-Zur, A., Fructman, A., Ashkenazy, J. and Gany, A., "Analysis of the steady-state axial flow in the Hall thruster", *Phys. Plasmas*, vol. 9, no. 10, 2002, pp.4363 -4374.

[77]Gulczinksi, F. S., and Gallimore, A. D., "Near-Field Ion Energy and Species Measurements of a 5-kW Hall Thruster," *Journal of Propulsion and Power*, Vol. 17, No. 2, 2001, pp. 418–427.

[78]King, L. B., and Gallimore, A. D., "Ion-Energy Diagnostics in the Plasma Exhaust Plume of a Hall Thruster," *Journal of Propulsion and Power*, Vol. 16, No. 5, 2000, pp. 916–922.

[79]Syage, J. A., "Electron Impact Cross Sections for Multiple Ionization of Kr and Xe," *Physical Review A*, vol. 46, 1992, pp. 5666–5680.

[80]Itikawa, Y., "Photon and Electron Interactions with Atoms, Molecules and Ions," 2003, Landolt-Börnstein, Vol. I/17, Subvolume C. Berlin, Germany: Springer.

[81]Freund, R. S., Wetzel, R. C., Shul, R. J., and Hayes, T. R., "Cross-section measurements for electron-impact ionization of atoms," *Physical Review A*, Vol. 41, No. 7, April 1990, pp. 3575-3595.

[82]Hayes, T., Wetzel, R., and Freund, R., "Absolute Electron-Impact-Ionization Cross-Section Measurements of the Halogen Atoms," *Physical Review A*, Vol. 35, No. 2, Jan. 1987, pp. 578–584.

[83]Raitses, Y., Smirnov, A., Staack, D., and Fisch, N. J., "The dependence of the electron temperature on the discharge voltage for different Hall thruster configurations," *Proceedings of the 29th International Electric Propulsion Conference*, Paper 2005-052, Oct.–Nov. 2005.